

Université du Québec  
Institut National de la Recherche Scientifique  
Center INRS-Institut Armand-Frappier

**Assessing Compound Self-aggregation in Drug Discovery and Development**

**By**

**Marwa Dlim**

Thesis submitted in partial fulfillment of the requirement of the degree of Master (M.Sc.) in  
Experimental Health Sciences

**Evaluation Committee**

President of the jury and  
Internal examiner

Pr Charles Calmettes  
INRS-Institut Armand-Frappier

External examiner

Pr Guillaume Lamoureux, Ph.D.  
Department of Chemistry and Biochemistry  
Concordia University, Montreal, QC

Research director

Pr Steven LaPlante, Ph.D  
INRS-Institut Armand-Frappie

## ACKNOWLEDGEMENTS

First and foremost, I would like to thank GOD Almighty for the wisdom, strength, peace of my mind and good health he bestowed upon me so that I could finish this research.

I would like to express my gratitude to my family for their constant encouragement, which helped me with the completion of this research. My brother, Anas, was always by my side when I needed him most. I send special thanks to my father, mother and sisters for motivating me to complete my graduate studies and for their enduring encouragement and support.

I would also like to thank my supervisor Prof. Steven LaPlante for welcoming me into his laboratory and for his support throughout my studies.

I also thank my advisor, Prof. Patric Labonte of the Virology and Immunology Department at Armand-Frappier INRS, and his Ph.D. student, Marwa Alkaber.

I would like to thank Jessy Tremblay in for his help, advice and invaluable information for all Confocal Microscopy experiments.

I also thank my friends who are always by my side, cheering me on. I especially thank Fatma Shahout for her help with this project especially in difficult times.

Lastly, I wish to express my gratitude to the Ministry of Education of Libya for financial support during my stay in Canada, and to NMX for their support.

## Abstract

When drug-like compounds are placed in aqueous media, it is commonly understood that they can solubilize and disperse into solution as lone-tumbling molecules and/or exist as solid precipitate. However, this simplistic biphasic view is no longer valid. Instead, a triphasic model better describes compound solution behavior where compounds can also adopt an intermediate phase where compound molecules self-associate into a range of assemblies that can resemble clusters, fibers, micelles and many other forms. Although the physicochemical parameters that dictate the features of these assemblies are not yet understood, it is clear that the nature of the triphasic equilibria profoundly affects a compound's properties, especially from the pharmaceutical perspective. We refer to these amazing assemblies as “nano-entities” and provide an introduction (Chapter 1).

This thesis aims to attract attention to these nano-entities which have, for the most part, gone undetected because they are invisible to the naked eye and detection strategies are seriously underdeveloped. We do so by first exploiting the nuclear magnetic resonance (NMR) aggregation assay that involves monitoring the solution behavior of a series of small-molecule dyes at various concentrations (see Chapter 2). This dilution-based assay demonstrates that some dyes can exist as single-molecule entities whereas others can adopt aggregates of distinct sizes. Interestingly, dyes with highly related chemical structures can adopt largely different sized aggregates - demonstrating the existence of structure-nanoentity relationships – which suggests that they can assume and/or be designed to have distinct properties. One property was evaluated where the drug Quetiapine (Seroquel) was added to the dye Congo red which resulted in the absorption of the drug into the dye nano-entity. This showed a direct drug-dye interaction, and it demonstrated that dye aggregates can have influence on drug solution behaviors. In summary, our studies demonstrate that the NMR aggregation assay can serve as a practical and valuable tool to monitor nano-entities and to better understand their associated properties (e.g. toxicity, off-target activity) and potential utility (e.g. drug encapsulation, drug delivery systems).

Chapter 3 further explores complementary strategies for detecting nano-entities. The goal was to develop, as much as possible, a combination of methods that could then be employed for correlating a compound's properties with its physicochemical and nano-entity behavior in solution. We use several anticancer drugs (Sorafenib, Lapatinib, Gefitinib and Fulvestrant) and an antileprosy drug (Clofazimine) as model systems to better understand their physicochemical behavior and self-association properties, and to explore various techniques for probing their three-state equilibria. Their behaviors in buffers, media and cells were monitored by a combination of NMR, dynamic light scattering (DLS), transmission electron microscopy (TEM), and confocal microscopy. These drugs were found to self-associate into relatively large nano-entities having distinct types and sizes that depend on the media. Furthermore, these compounds were capable of entering cells. Noteworthy advantages and “blind spots” were observed for the various detection techniques employed. It was concluded that a combination of methods is necessary to expose these drugs' elusive solution equilibria.

Our conclusion from the above work is that we have stumbled upon a great opportunity. Small molecules can form many types of nano-entities that depends on the media and conditions. These entities have properties – some undesired and others favorable. Our strategies can help the detection of the entities. The field is now open for exploitation purposes. For example, nano-entities could be used as drug encapsulation and drug delivery systems. This field is wide open and awaiting developments.

**Key words:** aggregation, promiscuity,

## TABLE OF CONTENTS

<b>ACKNOWLEDGEMENTS</b>	ii
<b>Abstract</b>	iii
<b>Table of Content</b>	v
<b>List of Figures</b>	vii
<b>List of Abbreviations</b>	viii
<b>CHAPTER 1: BRIEF INTRODUCTION</b>	9
1.1 Introduction to the Concept of Compound Aggregates and their Properties	10
1.2 Detection Methods of Compound Aggregation	13
1.3 Hypotheses	14
1.4 Objectives	14
1.4.1 Develop Effective Techniques for Detecting the Full Range of Nano-entities	14
1.4.2 Demonstrate the Ability of Small-Molecule Aggregation to Penetrate Cell Membrane and Investigate their Effect on Cell Proliferation	15
<b>CHAPTER 2: SCIENTIFIC ARTICLE (PUBLISHED)</b>	16
2.1 Presentation of Scientific Article	17
2.2 Contributions of the Authors	17
2.3 Supporting Information	25
<b>CHAPTER 3: SCIENTIFIC ARTICLE (TO BE SUBMITTED)</b>	27
3.1 Contributions of the Authors	28
3.2 <i>Revealing Drug Nano-entities</i>	29
3.3 Supporting Information	44
	v

<b>CHAPTER 4: RÉSUMÉ EN FRANÇAIS (French Summary)</b>	<b>61</b>
4.1 Introduction	62
4.2 Méthodes de Détection de l'agrégation de Composés	65
4.3 Hypothèse	67
4.4 Objectifs	67
4.4.1 Développer des Techniques Efficaces Pour Détecter l'ensemble des nano-entités	67
4.4.2 Démontrer la Capacité de l'agrégation de petites molécules à pénétrer dans la membrane cellulaire et étudier leur effet sur la prolifération cellulaire	67
<b>REFERENCES</b>	<b>69</b>

## LIST OF FIGURES

<b>Figure 1.</b> Compounds adopting a three-phase equilibrium	11
<b>Figure 2.</b> Proposed mechanism of inhibition and other properties of compound aggregates	12
<b>Figure 3.</b> Examples of the application of the “detergent effect” Tween 80.	14

## LIST OF ABBREVIATIONS

<b>Abbreviation</b>	<b>Full Designation</b>
<b>CAC</b>	Critical Aggregation Concentration
<b>CPMG</b>	Carr- Purcell-Meiboom-Gill
<b>CLSM</b>	Confocal Laser Scanning Microscopy
<b>DLS</b>	Dynamic Light Scattering
<b>FBS</b>	Fetal Bovine Serum
<b>HTS</b>	High-throughput Screening
<b>MST</b>	Magnetic Secure Transmission
<b>NMR</b>	Nuclear Magnetic Resonance
<b>PBS</b>	Phosphate Buffer Saline
<b>SAR</b>	Structure Activity Relationship
<b>SEM</b>	Scanning electron microscopy
<b>SPR</b>	Surface Plasma Resonance
<b>TEM</b>	Transmission Electron Micrograph.
<b>TPSA</b>	Total Polar Surface Area
<b>USEM</b>	Ultra-Thin Section Electron Microscopy

## **CHAPTER 1: BRIEF INTRODUCTION**

## 1.1 Introduction to the concept of compound aggregates and their properties

This thesis aims to alter the common biphasic view of the solution behavior of compounds to a more triphasic view that includes an intermediate aggregate phase. Figure 1 shows a triphasic view which features an intermediate state of soluble aggregates, keeping in mind that each compound has its own distinct equilibrium between the three states (LaPlante *et al.*, 2013). Aggregates can form spontaneously and reversibly in aqueous buffer through critical aggregation concentration (CAC) (Duan *et al.*, 2015; Irwin *et al.*, 2015). Each compound assumes its own fingerprint pattern within this triphasic model, which depends on solvent, media, concentration, temperature, pH, and many other factors. The existence of soluble aggregates, their variation of sizes and types, and their properties has long eluded detection and attention. Aggregation of small molecules can form at micromolar and even sub micromolar concentrations in aqueous media, while ranging from 50 to over 800 nm (Owen *et al.*, 2012). Moreover, aggregation is stable in the biological system media such as gastrointestinal tract and intestine as well as media with serum albumin (Tóth *et al.*, 2017) (Lu *et al.*, 2011). The previous work has often been rationalized based on the observations that typical drug compounds are highly serum-bound *in vivo* (Lu *et al.*, 2011). Because of this, the majority of a compound would be expected to be bound to serum proteins such as albumin, leaving compounds mostly unavailable to self-associate. This assumption is unfounded, in a previous study, involving an NMR aggregation test, it clearly shown that aggregating compounds remained self-associated in a range of pharmacology buffers, plasma and blood. This would suggest that there is a significant affinity for self-association for some compounds (LaPlante *et al.*, 2013).

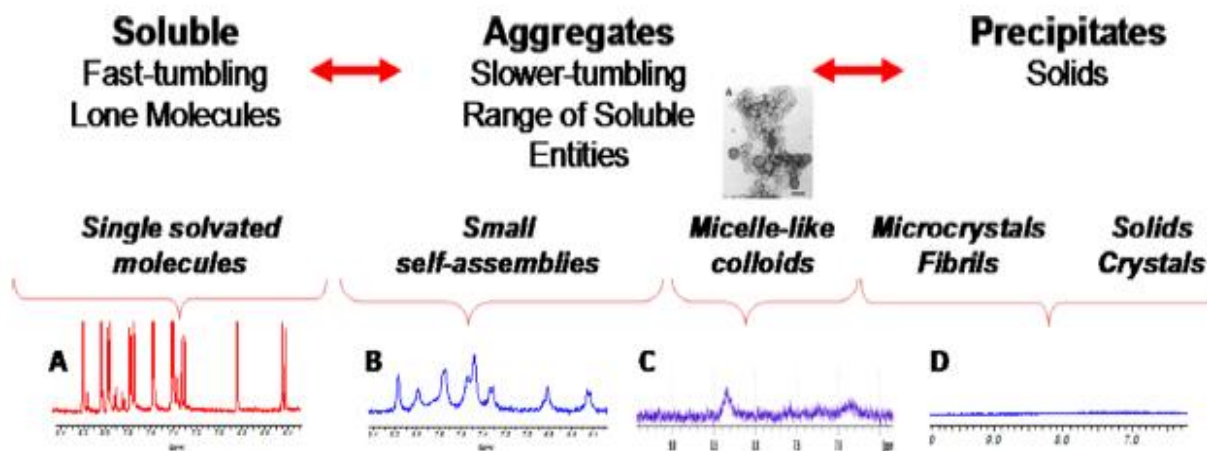


**Figure 1.** Compounds adopting a three-phase equilibrium when placed in aqueous media. At the bottom are  $^1\text{H}$  NMR spectra (600 MHz) of various compounds in a buffer (50 mM sodium phosphate pH 7.4) at nominal concentrations of 200  $\mu\text{M}$ , (LaPlante *et al.*, 2013).

Aggregates can have peculiar properties which act on a non-targeted spot and can change the results. One of these properties is false positive result which could be related to chemical reactivity, high molecular flexibility, and the hydrophobicity of the compound. (Feng *et al.*, 2005). In addition, structural activity relationship (SAR) could also contribute to this phenomenon. For instance, some dyes with highly related structure can adopt a very different sized aggregate (Murugesan *et al.*, 2018). The previous research also reported that aggregation can cause false positive results through promiscuous inhibition (Irwin *et al.*, 2015). Other research on the topic suggests that aggregates have properties that can have serious impacts along the drug discovery pathway. For example, a systematic study showed that 95% of the hits from a high-throughput screen were eliminated as false-positives due to compound aggregates (Feng *et al.*, 2007). However, studies thus far have just begun to correlate the existence of nano-entities with this promiscuity such as drug toxicity, and hyper-bioavailability. They can lead to nonspecific interactions with various proteins, and influence structurally and functionally unrelated proteins leading to unreliable false positive screening assays. In fact, some drug-like molecules inhibit many different enzymes. However, studies were performed on these mechanisms and there is still a population of nonspecific enzyme inhibitors which are poorly understood. It was previously discovered that unrelated promiscuous molecules share several unusual properties, such as time-

dependent behavior, steep inhibition curves, sensitivity to enzyme concentration and ionic strength. To account for this behavior, it has been suggested that these compounds share the capability of forming aggregates at micromolar concentrations in aqueous solution, and that the inhibiting of various enzymes is caused by these aggregate species (Seidler *et al.*, 2003), leading to false positive “hits” in biochemical assays. Nonetheless, precisely how aggregates cause non-specific inhibition remains poorly understood. Possible mechanisms of action which elucidate aggregate-based inhibition are shown in (Figure 2).

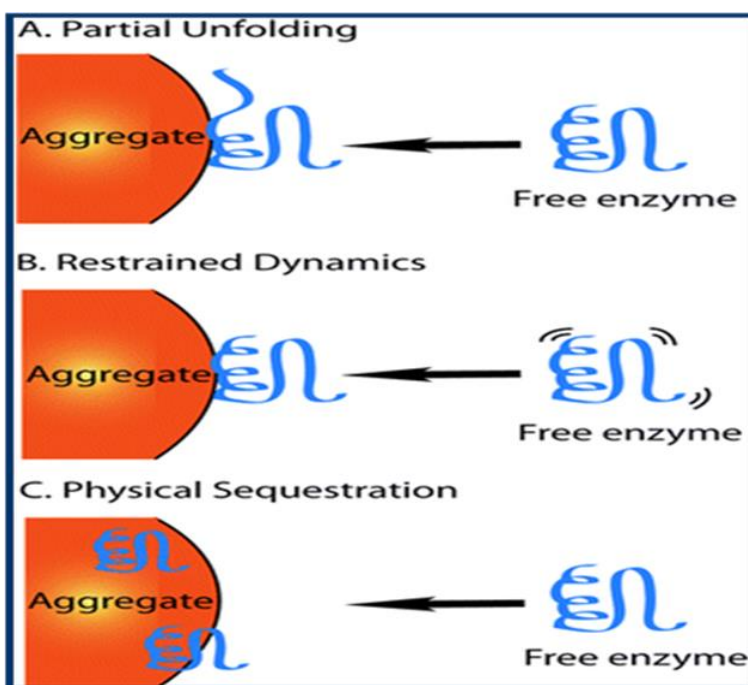


**Figure. 2.** Proposed mechanism of inhibition and other properties of compound aggregates (Coan *et al.*, 2009).

## 1.2 Detection methods of compound aggregation

Several computational methods and biophysical tests are currently used to detect small molecule aggregates in aqueous solution. One of the most common methods is enzyme-based inhibition assays such as lactate dehydrogenase,  $\beta$ -lactamase and chymotrypsin (Chan *et al.*, 2009) that are widely used to identify aggregation by measuring the absorbance of enzymatic reaction products based on colorimetric change in solution. With the existence of aggregation and nonspecific protein inhibition, there could be alteration in the enzymatic reaction ratio and in reaction kinetics. In addition, the colorimetric changes give direct observation and readouts of enzymatic activity. However, the absorbance of small molecules can influence the absorbance output signal without respect for their potential aggregation. Other common methods including dynamic light scattering (DLS), a comparatively straightforward detection method currently used to evaluate the size of compound aggregates suspended in a solution by determining the time-dependent temporal fluctuations and scattering intensity (Chan *et al.*, 2009). DLS could be sensitive to large aggregates but is less ideal for determining small entities, and some researchers believe that differentiating aggregates from precipitant using this assay is really difficult. Surface plasmon resonance (SPR) is another aggregate detection method has been recently used on an optical biosensor surface, SPR is more reliable compared with enzymatic inhibition or DLS methods due to its direct affinity measurement of the molecules observed.

Very recently, compound self-aggregations in aqueous media have been detected by using  $^1\text{H}$  NMR-based assay through various dilution experiments. By using this assay, eliminating self-aggregate molecules from fragment screening libraries would be more straightforward. A high number of small molecules are affected by aggregation which exist more likely at high concentrations (LaPlante *et al.*, 2013). As previously described, when a compound in aqueous media, it is assumed to adapt equilibria between three various phases including solid forms, soluble single molecules and soluble aggregate entities. Each individual phase of these three states can be significantly identified by  $^1\text{H}$  NMR. It is noted that several compounds display normal  $^1\text{H}$  NMR spectra, whereas others display unusual spectra. Moreover, NMR resonances could be either sharp or broad according to the tumbling aggregate behaviors of each state. A sharp NMR resonance is expected to be observed for soluble single molecules due to their fast-tumbling behaviors. On the other hand, solid forms that behave slow tumbling abilities can be also detected using NMR

spectrum but requires breaking the aggregates into smaller entities using detergents for detection purposes, (see Figure 3) (LaPlante *et al.*, 2013).

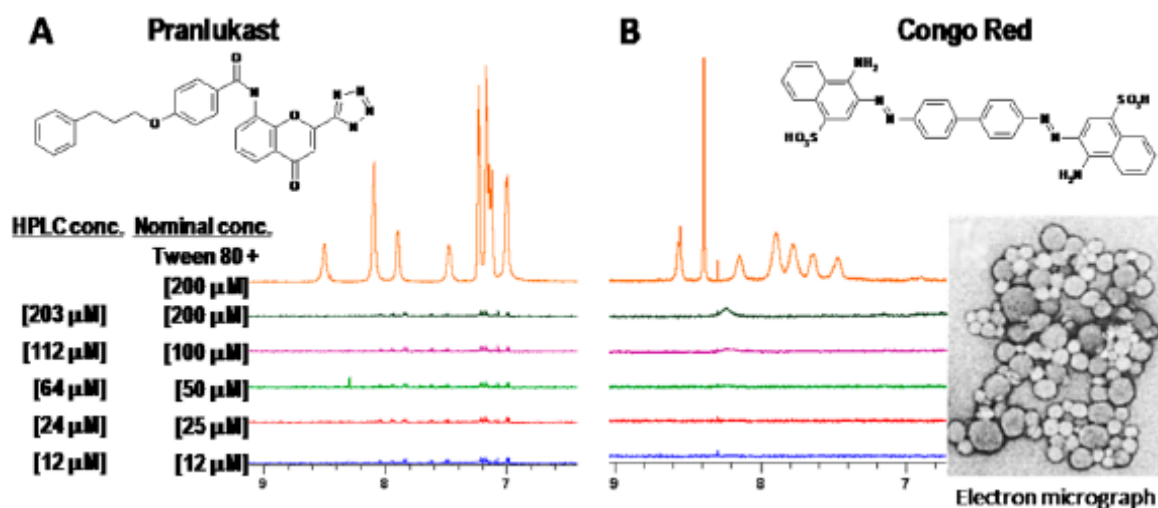


**Figure 3** Examples of the application of the “detergent effect” Tween 80. Shown  $^1\text{H}$  NMR spectra of two compounds Pranlukast and Congo Red in aqueous solution at various concentrations. The buffer employed for these studies was 50 mM sodium phosphate pH 7.4 in 100%  $\text{D}_2\text{O}$  solvent, (LaPlante *et al.*, 2013).

### 1.3 Hypothesis

The hypothesis of this study is that many types of drug nano-entities exist and are detectable. Also, several different types of drug and dye molecules undergo the aggregation process and have the ability to penetrate cells.

### 1.4 Objectives

#### 1.4.1 Develop effective techniques for detecting the full range of nano-entities

We first develop a series of accessible and complementary aggregation assays and strategies. To do so, scientific tools must be systematically evaluated, with the goal of enabling the detection of the full range of nano-entity types and sizes. Because each technique has its strengths and “blind spots”, we intend to acquire data on a training set of compounds that are known to be either aggregators or non-aggregators. Furthermore, in order to properly observe and characterize the small-to-intermediate-sized aggregates, a variety of NMR tools have been explored ( $^1\text{H}$  NMR aggregation assays) that are amenable to high-throughput screening. Although not ideal, very large NMR-invisible aggregates can be exposed and observed by  $^1\text{H}$  NMR via disruption upon the

addition of detergents. Other alternatives for directly observing large aggregates include dynamic light scattering techniques (DLS), which can report the sizes of large aggregates but are impractical for aggregate mixtures and small aggregates. Thus, because electron microscopy can provide detailed visual information on large aggregates (sizes and types), this approach has been employed for selected compounds.

#### **1.4.2 Demonstrate the ability of small-molecule aggregation to penetrate cell membrane and investigate their effect on cell proliferation**

Little is known of how aggregates enter the cell, although some hypotheses have been proposed. We run experiments to gain insight into how aggregates exist inside cells, the results of which should then shed light on their mechanism of action. This objective evaluated the impact of aggregates entering cells and nuclei or permeating membranes and affecting organelles. Toxicity response properties were also evaluated. Confocal microscopy was conducted to detect the fluorescent compounds aggregates. By applying this approach, we could see the aggregation inside cells, nuclei and cytoplasm.

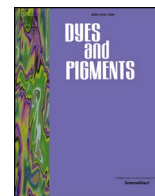
## **CHAPTER 2: SCIENTIFIC ARTICLE (PUBLISHED)**

## **2.1 Presentation of scientific article**

The results in this research study illustrate that some dyes can exist as single molecules, whereas others can adopt aggregates in different sizes. In addition, dyes with highly related structures exhibit differently-sized aggregates, also show drug-dye interaction and how dye aggregates can affect drug solution behaviour. The results are presented in the form of a scientific article published in the February 21, 2018, edition of The *Journal of Dyes and Pigments* (volume 153, Pages 300-306, DOI.ORG/10.1016/j.dyepig), a periodical with an impact factor of 3.767.

## **2.2 Contributions of the authors**

The research work presented in this scientific article was conducted by Jayadeepa R. Murugesan, Fatma Shahout and Marwa Dlim, which are students in Steven LaPlante's lab. Marwa Dlim was involved in several of the scientific and intellectual steps of the work. The first drafts of the Abstract, Introduction, and Materials and Methods sections were written by Marwa Dlim, who also contributed in prepared the figures, and participated in the electron micrograph (TEM) testing stage, NMR samples preparation and data acquisition. Dr. Pat Forgione of Concordia University participated in the preparation of this manuscript, reviewing most of the writing sections. Dr. Steven LaPlante supervised the work and contributed to the NMR analysis, the interpretation of the data, and the design of the figures.



## Revealing dye and dye-drug aggregation into nano-entities using NMR

Jayadeepa R. Murugesan<sup>a</sup>, Fatma Shahout<sup>a</sup>, Marwa Dlim<sup>a</sup>, M. Michele Langella<sup>b</sup>,  
Ernesto Cuadra-Foy<sup>b</sup>, Pat Forgiione<sup>b,\*\*</sup>, Steven R. LaPlante<sup>a,\*</sup>

<sup>a</sup> Université du Québec, INRS-Institut Armand-Frappier, 531, Boulevard des Prairies, Laval, Québec H7V 1B7, Canada

<sup>b</sup> Concordia University, Department of Chemistry and Biochemistry, 7141 rue Sherbrooke O., Montreal, Québec H4B 1R6, Canada

### ARTICLE INFO

#### Keywords:

Dye  
Drug  
Aggregation  
NMR  
Nano-entities  
Colloids  
SNR

### ABSTRACT

It is becoming increasingly apparent that small molecules can self-assemble into a wide-range of nano-entities in solution that have intriguing properties. The recently introduced NMR aggregation assay is playing an important role in revealing these nano-entities. Here, we employ the NMR aggregation assay to expose the self-aggregation tendencies of dyes in solution. This dilution-based assay demonstrates that some dyes can exist as single-molecule entities whereas others can adopt aggregates of distinct sizes. Interestingly, dyes with highly related chemical structures can adopt largely different sized aggregates - demonstrating the existence of structure-nanoentity relationships (SNR) – which suggests that they can assume and/or be designed to have distinct properties. One property was evaluated where the drug Quetiapine (Seroquel) was added to the dye Congo red which resulted in the absorption of the drug into the dye nano-entity. This showed a direct drug-dye interaction, and it demonstrated that dye aggregates can have influences on drug solution behaviors. The NMR method described in this study provides a practical and valuable tool to monitor dye aggregates and to better understand their associated properties (e.g. toxicity, off-target activity) and potential utility (e.g. drug encapsulation, drug delivery systems).

### 1. Introduction

Small molecules can assume a wide range of behaviors in solution that can be considered within the context of a tri-phasic equilibrium [1,2]. That is, when a compound is placed in aqueous solution it can equilibrate between at least three states (Fig. 1). Some of the molecules can exist as soluble, fast-tumbling lone molecules that are completely diffuse, whereas others can form solid precipitate(s), and others can self-associate and adopt intermediate soluble aggregates or nano-entities. Notably, each compound likely has its own unique equilibrium signature and relative population among these states, and there is a critical dependence on many other factors such as buffer, co-solutes, etc.

The detection and quantification of a compound's signature equilibrium remains elusive to this day [2]. Whereas the solid precipitate phase is detected visually (or via a microscope for fibrils), the distinctions between the soluble lone-molecules and aggregate phases are not apparent. This is in part due to the limited detection methods available such as dynamic light scattering (DLS) [3]. DLS is a practical technique that can reveal the existence of large, micelle-like aggregates that are homogeneous. However, we recently introduced an NMR aggregation

assay that exposed a wide range of nano-entity sizes that can exist [1,2] especially small multimers, which are often undetectable by DLS. Fig. 1 shows how NMR is sensitive to compound tumbling rates and behavior for all three phases. That is, fast tumbling molecules exhibit sharp resonances (Fig. 1A), and solid precipitates result in extremely broad and unobservable resonances by solution NMR (Fig. 1D). Aggregates give rise to intermediate resonance attributes such as broad resonances and/or unusual features such as those shown in Fig. 1B and C. Thus, we chose to employ NMR in this study to explore the behavior of dyes in solution, which could then be a valuable tool to begin correlating with their properties. Here, we demonstrate that the NMR aggregation assay is a feasible method to explore the behavior of dyes in solution, which can then be a practical tool for correlating nano-entity properties.

### 2. Materials and methods

#### 2.1. Compounds - dyes

The dyes and drug used in this study were all obtained from commercial vendors. The dyes and their CAS numbers are as follows: Azo Rubine (3567-69-9), Acid Blue 9 (3844-45-9), Erythrosin B (16423-68-

\* Corresponding author.

\*\* Corresponding author.

E-mail addresses: [pat.forgione@concordia.ca](mailto:pat.forgione@concordia.ca) (P. Forgiione), [steven.laplante@iaf.inrs.ca](mailto:steven.laplante@iaf.inrs.ca) (S.R. LaPlante).

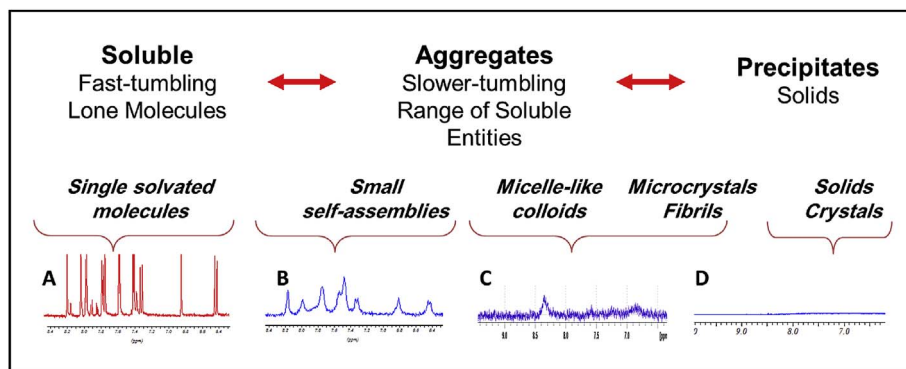


Fig. 1. Compounds can adopt a three-phase equilibrium when placed in aqueous media. On the bottom are  $^1\text{H}$  NMR spectra (600 MHz) of various compounds in buffer (50 mM sodium phosphate pH 7.4) at nominal concentrations of 200  $\mu\text{M}$ .

0), Allura Red (25956-17-6), Fast Green (2353-45-9), Erochrome Blue Black B (3564-14-5), Naphthol Yellow (846-70-8), Sudan II (3118-97-6), Acid Violet (1694-09-3), Indigo carmine (860-22-0), Methylene blue (61-73-4), Tartrazine (1934-21-0), Solvent Orange 2 (2646-17-5), 4,4'-(9-Fluorenylidene)dianiline (15499-84-0), 4-((4-hydroxy-1-naphthalenyl)azo)benzenesulfonic acid, monosodium salt (523-44-4), Fast Green (2353-45-9), Quetiapine fumarate (111974-72-2). All were purchased from TCI whereas Acid Green (3087-16-9) and Patent Blue (3536-49-0) were purchased from Chem-Imp.

## 2.2. NMR sample preparation

Powder dyes were weighed and appropriate amounts placed in Eppendorf tubes followed by the addition of deuterated DMSO to form 20 mM dye stock solutions, as described in Fig. 2. The buffer used for preparing the NMR samples was 50 mM sodium phosphate pH 7.4 in

100%  $\text{D}_2\text{O}$ . When preparing the aggregation buffer, note that a pH of 7.8 corresponds to a pH of 7.4. Tween 80 stock (10% vol/vol in above buffer) was added to samples as defined in the procedure provided below. Further details on how samples were prepared are provided in Fig. 2.

## 2.3. NMR experiments

The pulse programs for the NMR aggregation assay are the standard one-dimensional  $^1\text{H}$  NMR experiments available on all commercial spectrometers. There are several optional parameters that can be modified if desired. Given that the buffer consists of 100%  $\text{D}_2\text{O}$ , one can choose to use a standard  $^1\text{H}$  NMR pulse program or one that includes solvent suppression. The latter may be desirable if large  $\text{H}_2\text{O}$  resonance peaks exist due to the hygroscopic property of deuterium oxide. The experiments shown here were run on a 600 MHz Bruker AV III NMR

## Sample Preparation for NMR Aggregation Assay

### Required Supplies:

- Aggregation Buffer:
  - 50 mM sodium phosphate pH 7.4 in 100%  $\text{D}_2\text{O}$
- Tween 80 stock (10 % vol/vol in above buffer)
- 7 Eppendorf tubes
- 2 Pipettes: 2 – 20  $\mu\text{L}$  and 200 – 1000  $\mu\text{L}$

### Calculation for 20 mM compound stock solution:

X = exact mass weighed in mg (0.3 – 0.6 mg)

Y = MW of your compound

Z = volume of  $\text{DMSO-d}_6$  to be calculated / added

$$\frac{X \text{ mg}}{Y \text{ mg/mmol}} = Z \text{ mL} \quad \left\{ \begin{array}{l} \text{Volume should work} \\ \text{out to 20 – 200 } \mu\text{L} \end{array} \right.$$

0.02 M

### A- Prepare 20 mM compound stock solution (as above)

### B- Portion out aggregation buffer

- 1500  $\mu\text{L}$  in tube 5
- 500  $\mu\text{L}$  in each of tubes 1-4

### C- Add/mix 15 $\mu\text{L}$ of above 20 mM compound stock to tube 5

- This tube now becomes the 200  $\mu\text{M}$  stock solution
- If precipitate forms, take note and proceed

### D- Transfer 500 $\mu\text{L}$ of the 200 $\mu\text{M}$ stock solution to tube 6.

### E- Take 500 $\mu\text{L}$ of the 200 $\mu\text{M}$ stock and add to tube 4

- Mix with the 500  $\mu\text{L}$  buffer already present
- This becomes first 2x dilution
- Transfer 500  $\mu\text{L}$  from tube 4 to tube 3. Mix.
- Repeat dilution and mixing for tube 2 then 1.

### F- Lightly centrifuge tube 6 (2,000 rpm 10 minutes).

Transfer precipitate-free supernatant to a spare tube

### G- Add/Mix 8 $\mu\text{L}$ of Tween 80 stock solution to a spare tube

### H- Transfer solution from tubes 1-5 and spare tube to separate NMR tubes

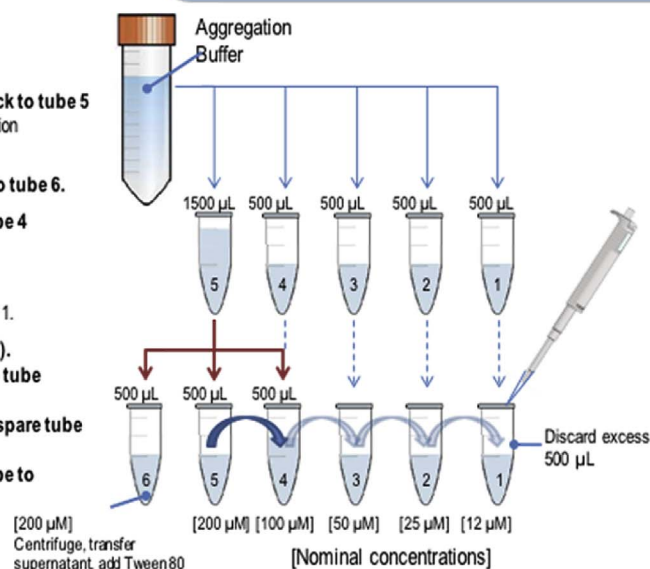


Fig. 2. Detailed procedure for preparing samples for the NMR aggregation assay [1,2].

equipped with a sample changer. The number of scans was typically 256 scans, with a relaxation delay plus acquisition time of 2s, which ensured that all samples for each compound could be, acquired overnight using a sample changer. Data visualization and interpretation are also simple. For the work described here, Bruker's TOPSPIN software allows for the facile superposition of 1D NMR spectra along with zooming capabilities. Other software from ACD and other vendors also allow for spectral superpositions. Instant JChem for Office Version 18.3.0 was used for chemical structure handling, data analyzing, visualizing and reporting capabilities within the Microsoft Office environment Chemaxon (<https://www.chemaxon.com>) [4].

#### 2.4. Electron microscopy

Congo red was diluted in DMSO with 50 mM sodium phosphate pH 7.4 in 100% D<sub>2</sub>O, and was prepared at 600 μM. Briefly, 100 μL of the sample was transferred into a 240 μL Airfuge tube. A carbon coated copper grid was inserted into the bottom of Airfuge tube with fine tweezers and centrifuged for 5 min at 20 psi. With tweezers, the carbon grid was gently removed and washed with distilled water for 1 min. The carbon grid was then negatively stained with 3% of phosphotungstic acid (PTA-3) for 1 min. The grid was then removed and blotted to dry with a bibulous paper and examined with a transmission electron microscope (Hitachi H-7100). The photographs were processed with the digital camera AMT version 600.147.

### 3. Results and discussion

#### 3.1. Detection of aggregation using <sup>1</sup>H NMR spectra as a function of dye concentration

The NMR aggregation assay involves the acquisition and monitoring of <sup>1</sup>H NMR spectra as a function of compound concentration. For single molecules that do not aggregate, each dye molecule is distal to one another, tumbles freely and is not affected by dilution. Sharp resonances are expected at all concentrations and do not shift left or right. Also, there should be no changes in the number and shape of the resonances (Fig. 3). The only changes expected are the resonance intensities as a function of concentration. For dyes that aggregate the molecules self-associate at higher concentrations, upon dilution they become more distal and tumble more freely. As a result, unusual NMR features and changes are expected due to changes in local environments (Fig. 3).

#### 3.2. NMR assay on structurally different dyes

Fig. 4 displays the <sup>1</sup>H NMR spectra as a function of concentration for Tartrazine, Methylene blue and Congo red. An overview of the spectra for Tartrazine suggests that the data is consistent with the predominance of the non-aggregating phase consisting of lone-molecules tumbling rapidly in solution. A single set of resonances exist which are sharp at all concentrations and are well-aligned (no shift left nor right). Furthermore, the addition of Tween 80 had no effect on the resonances intensities, which is expected in the absence of large, micellar aggregates. Electron microscopy also shows no signs of aggregates (Fig. 4).

Alternatively, Methylene blue and Congo red exhibit unusual spectral trends that are consistent with the observation of aggregates. Upon increasing the concentration of Methylene blue, the resonances shift significantly indicating changes in local environments upon self-association. These nano-entities are relatively small given the fact that resonances are observed, likely multimeric forms. This is in stark contrast to the observations made for Congo red. No sharp resonances are readily observed at all concentrations, despite exhibiting full solubility (clear solution, precipitate-free). Thus, Congo red self-assembles into very large nano-entities that result in extremely broad, unobservable

resonances. A closer look at the 200 μM concentration shows very broad peaks (*vide infra*), which become much sharper but nonetheless relatively broad upon addition of Tween-80. This latter observation suggests that Tween 80 partially breaks apart the Congo red aggregates into smaller entities that are finally observable as shown in Fig. 4. Congo red was also reported [5–7] to form large aggregates and here we show this by scanning electron microscopy (see electron micrograph on the top right of Fig. 4).

The scope of the current study was expanded to other classes of dyes, naphthol yellow S hydrate, Erythrosine B and 4, 4'-(9-fluorenylidene) dianiline (Fig. 5). Naphthol yellow S (hydrate) exhibited sharp resonances with no shift changes upon increasing the concentration, which is consistent with this dye behaving predominantly as a non-aggregator. For Erythrosine B and 4,4'-(9-fluorenylidene) dianiline, unusual features were observed in <sup>1</sup>H spectra of the NMR assay that were consistent with self-assemblies. <sup>1</sup>H NMR signals shifted right at higher concentrations of Erythrosine B, and resonances of 4,4'-(9-fluorenylidene)dianiline were only notable upon addition of Tween 80.

Other types of dyes were also evaluated (see Supporting Information, Figs. S1–S2). For example, Fig. S1 shows that Acid blue 9, Evans blue, and Indigo carmine also form distinct types of nano-entities. In the spectra of Acid blue 9, the <sup>1</sup>H NMR signals appear as expected for a non-aggregator, except that additional small resonances appear at higher concentrations. More apparent and unusual features are noted in the spectra of Evans blue and Indigo carmine.

#### 3.3. NMR assay on structurally similar dyes - Triarymethane class

We next explored the aggregation tendencies of a series of similar compounds. Overall, it was noted that dyes of the same class with subtle structural differences can show completely different aggregation tendencies. This is exemplified in Fig. 6 for three triarylmethane dyes (Patent blue, Light green SF yellowish and Acid violet 49). On one hand, the spectra of the Patent blue appears such that no aggregation is observed since no changes in the resonance number, shape and chemical shift occurs at the various concentrations. However, the spectra of Light green SF yellowish and Acid violet 49 display notable unusual trends. The resonances of Light green SF Yellowish exhibit shifts and the presence of two sets of peaks, which is indicative of the presence of more than one type of aggregate species. Broad resonances are observed for Acid Violet 49. These findings are consistent with the literature of cyanine dyes that are reported to adopt J and the H aggregates (bathochromic shift and hypsochromic shift in the absorption spectra, respectively) [8].

Perhaps the latter two dyes tend to aggregate as a result of π-π stacking interactions of the planar solvophobic aromatic rings [9], whereas Patent blue has the tetrahedral sulfonate groups in both the *ortho* and *para* positions of a phenyl ring that could prevent such π-π interactions. For Light green SF yellowish and Acid violet 49, the substituents are far away from the aromatic system (*para*) which may minimize steric influences and allow self-assembly.

#### 3.4. NMR assay on structurally similar dyes - Azo dyes with one phenyl and one naphthyl and bis-naphthyl group

The aggregation tendencies of another series of structurally related dyes was explored to see if the above observations were specific to one series or general. Fig. 7 displays the NMR data for three structurally-related azo dyes (Sunset yellow, Allura red and Orange II). In this case, all three compounds have unusual <sup>1</sup>H NMR spectral tendencies. The resonances of Sunset yellow are sharp but shift as a function of higher concentration – which is consistent with the existence of small nano-entities and literature reports using other spectroscopic studies [10–12]. For Allura red, the spectra contain both sharp and broad resonances indicating the presence of a mix of multiple aggregate types. On the other hand, the spectra for Orange II are consistent with the

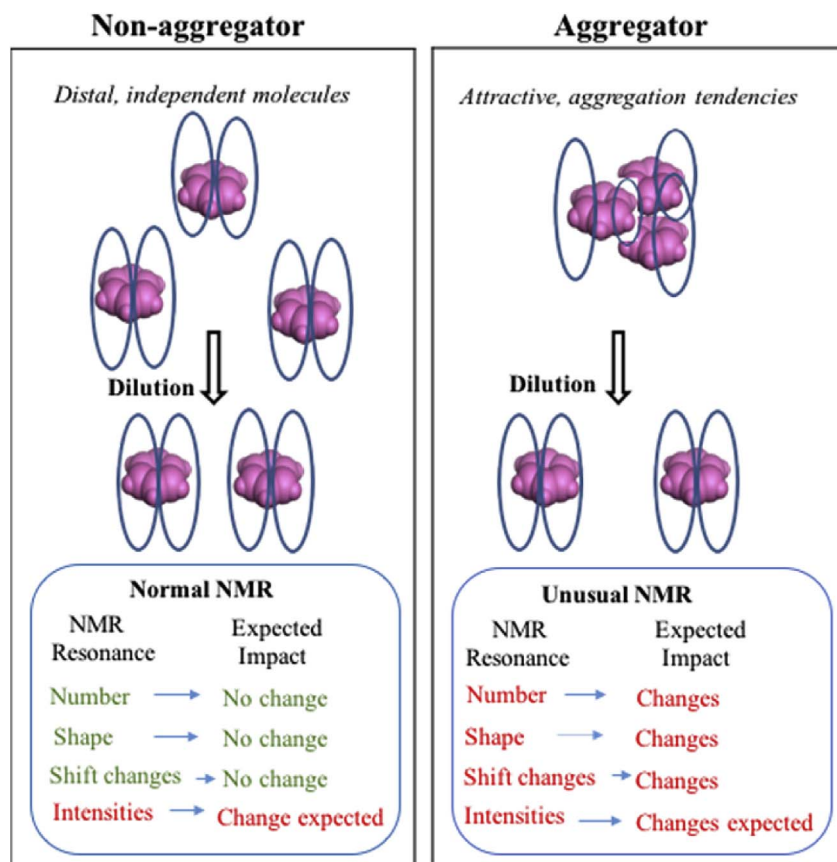


Fig. 3. Overview of the expected observations of NMR spectra and resonances upon dilution for dyes that aggregate versus those that do not in solution.

presence of very large nano-entities given that resonances only become apparent upon the addition of detergent. Clearly, these results suggest that structure-aggregate relationships exist and that the sulfonate anions play a more complex role beyond the simple expectation of enhancement of solubility [13].

The structure-aggregation relationships exposed above was then expanded to the structurally similar bis-naphthyl azo dyes that also have a different number of sulfonate anions. Fig. 8 reports the <sup>1</sup>H NMR spectra of Acid red 18, Amaranth and Eriochrome blue black B. A single set of resonances of Acid red 18 are observed and sharp throughout the concentration range, although there are some notable resonance shifts at higher concentrations. More dramatic shifts are found for Amaranth that is a regioisomer of Acid red 18. Perhaps the less pronounced

aggregate behavior is notable for Acid red 18 due to a suppression of  $\pi$ - $\pi$  stacking interactions given the proximity of the sulfonate groups to both naphthyl rings, as compared to Amaranth where the sulfonate anions lie at the periphery of the rings. The spectra of Eriochrome blue black B have truly unusual features with many sharp resonances that are inconsistent with a single species.

### 3.5. Dye-drug interactions

Dyes are used in a wide range of applications, including foods, drinks, cosmetics, tooth paste, medications. etc., Thus, a question worth addressing is whether dyes can interact directly with medical drugs that are also highly prescribed in our society. If so, there may be a potential

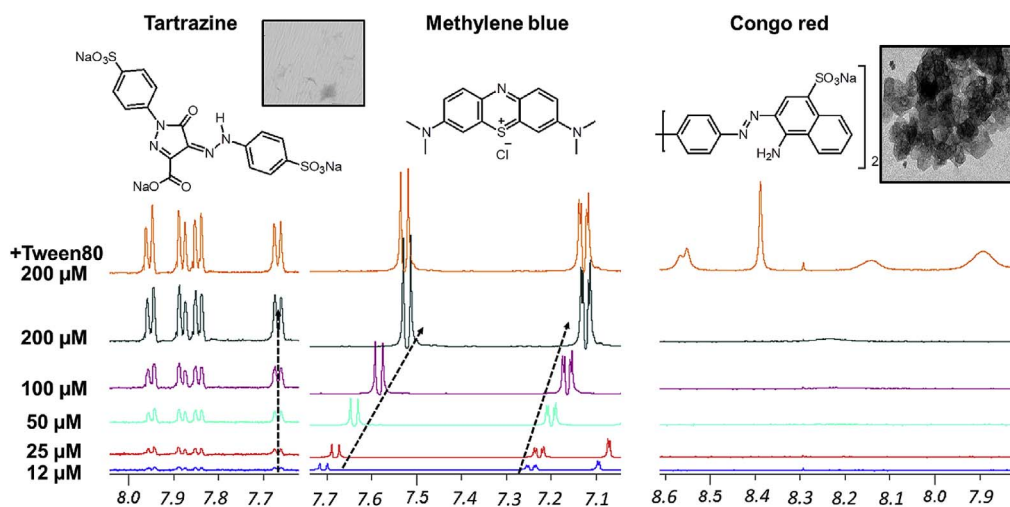


Fig. 4. NMR aggregation assay showing <sup>1</sup>H NMR spectra of three structurally different dyes obtained by dilution from 200  $\mu$ M to 12  $\mu$ M. Data displayed for Tartrazine (left), Methylene blue (middle) and Congo red (right). The insets on the top-right and left are electron micrographs of Congo red and Tartrazine in solution, respectively. (For interpretation of the references to color in this figure legend, the reader is referred to the Web version of this article.)

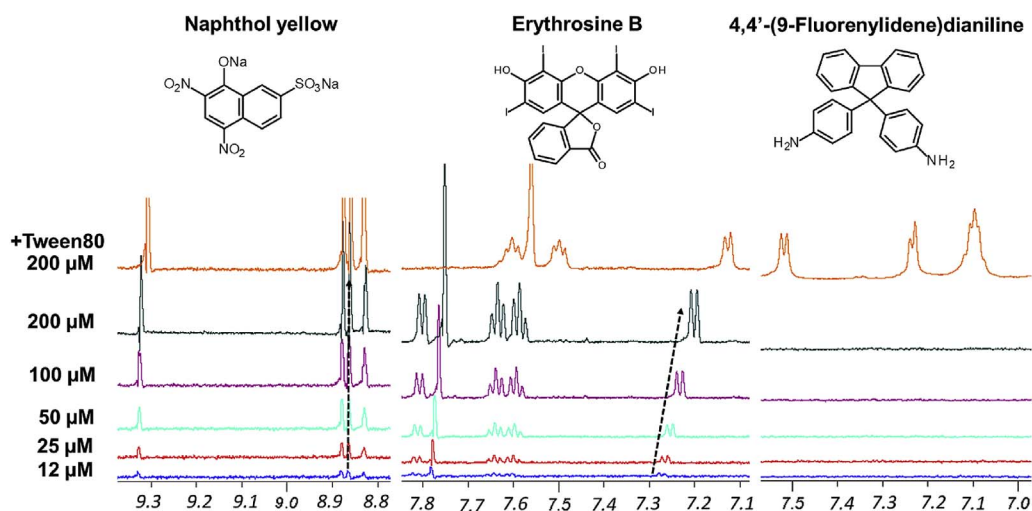


Fig. 5. NMR aggregation assay showing  $^1\text{H}$  NMR spectra of three structurally different dyes obtained by dilution from  $200\ \mu\text{M}$  to  $12\ \mu\text{M}$ . Data displayed for Naphthol yellow (left), Erythrosine B (middle) and 4,4'-(9-fluorenylidene)dianiline (right). (For interpretation of the references to color in this figure legend, the reader is referred to the Web version of this article.)

that dyes can compromise the intended medical use of certain drugs. Unfortunately, there have been few reports on drugs and other chemicals interacting with dyes to produce undesired effects [14], and as a result a detailed molecular view is lacking.

To illustrate how potential interactions can be studied using NMR, Congo red was added to Quetiapine and the NMR spectrum observed. Quetiapine is an antipsychotic drug used for the treatment of schizophrenia and bipolar disorder. The NMR spectrum of Quetiapine alone in Fig. 9 shows sharp resonances that are consistent with a non-aggregator behavior in solution. Congo red, which was used in the cellulose industry before it was banned for toxicity reasons, exhibits very broad resonances in Fig. 9 that is consistent with a behavior as an aggregator in solution. When mixed together, the broad resonances of Congo red remain whereas the resonances of Quetiapine become significantly broad. Based on this, it is apparent that Quetiapine interacts with Congo red and adopts its slow tumbling behavior as an aggregate. It also shows the potential impact that aggregates can have on other small molecules. Moreover, this provides a new tool for studying drug-dye or drug-drug interactions.

### 3.6. Discussion on dyes, solution behavior and properties

Dyes play an important role in our society, and are used in many products. They are produced in extremely large quantities world-wide for applications in various industries. For example, the clothing industry employs dyes to enhance marketability of their products. Also, the food industry employs color to enhance the attractiveness of their products. As a result, consumers are heavily exposed to small-molecule dyes that are worn and ingested, despite the fact that relatively little is known about their *in vivo* behavior, properties and toxicity. The impact on the environment is also significant. Effluents from the dye industry are eventually discharged into the environment as pollutants. Some can be readily degraded, but others, such as azo dyes are persistent as a result of their lipophilic nature. When the latter is degraded, azo dyes are well known to be susceptible to anaerobic reduction, releasing amines and hydrazine that can be carcinogenic [15]. Thus, dyes are highly prevalent in our society and their properties need to be investigated with appropriate tools.

Here, we introduce an NMR aggregation assay and found that some dyes tend to behave as lone single molecules in solution whereas others adopt nano-entity features. It is interesting that we also demonstrated

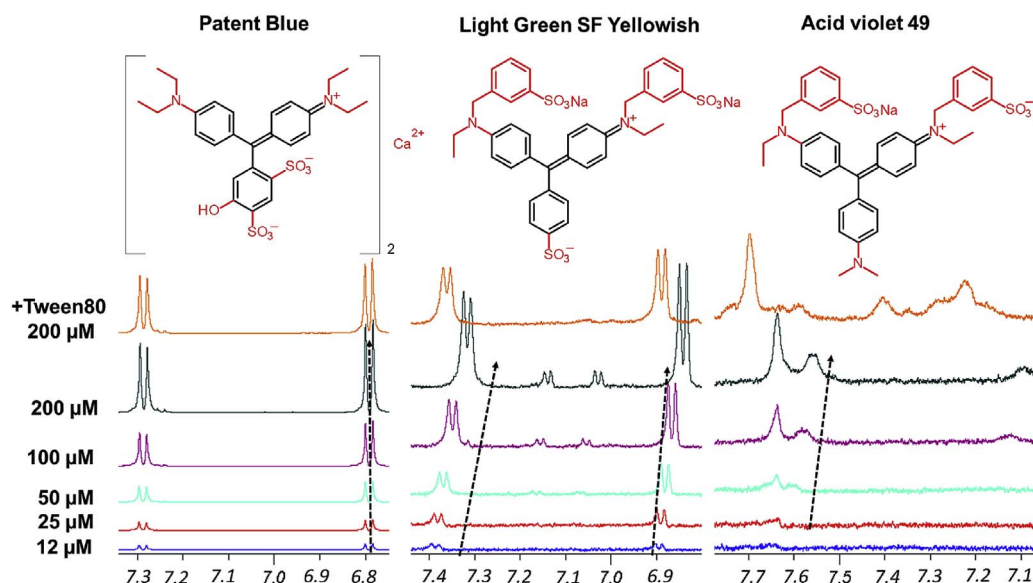


Fig. 6. NMR aggregation assay showing  $^1\text{H}$  NMR spectra of three structurally similar triarylmethane dyes obtained by dilution from  $200\ \mu\text{M}$  to  $12\ \mu\text{M}$ . Patent blue (left), Light green SF yellowish (middle) and Acid violet 49 (right). (For interpretation of the references to color in this figure legend, the reader is referred to the Web version of this article.)

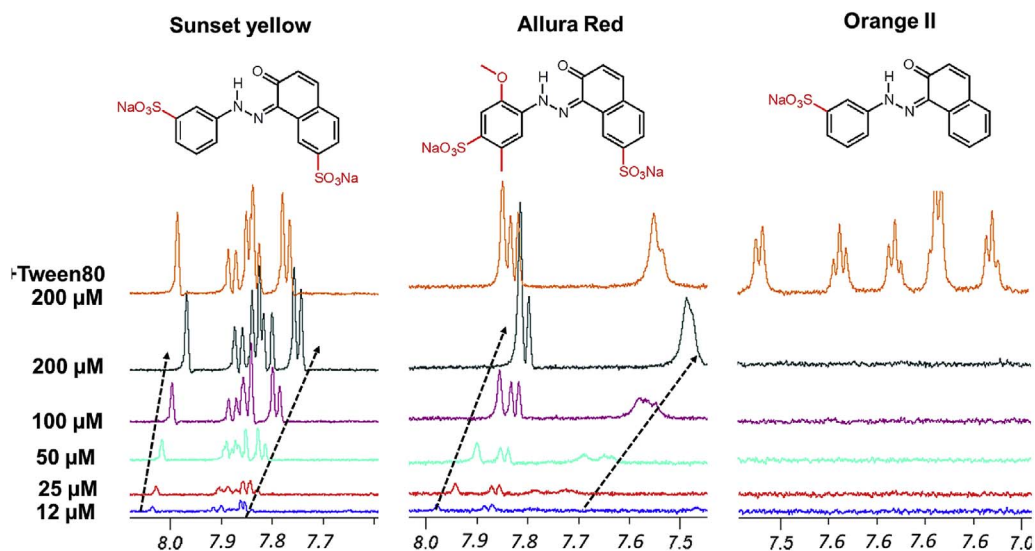


Fig. 7. NMR aggregation assay showing <sup>1</sup>H NMR spectra of three structurally similar azo dyes obtained by dilution from 200 μM to 12 μM. Sunset yellow (left), Allura red (middle) and Orange II (right). (For interpretation of the references to color in this figure legend, the reader is referred to the Web version of this article.)

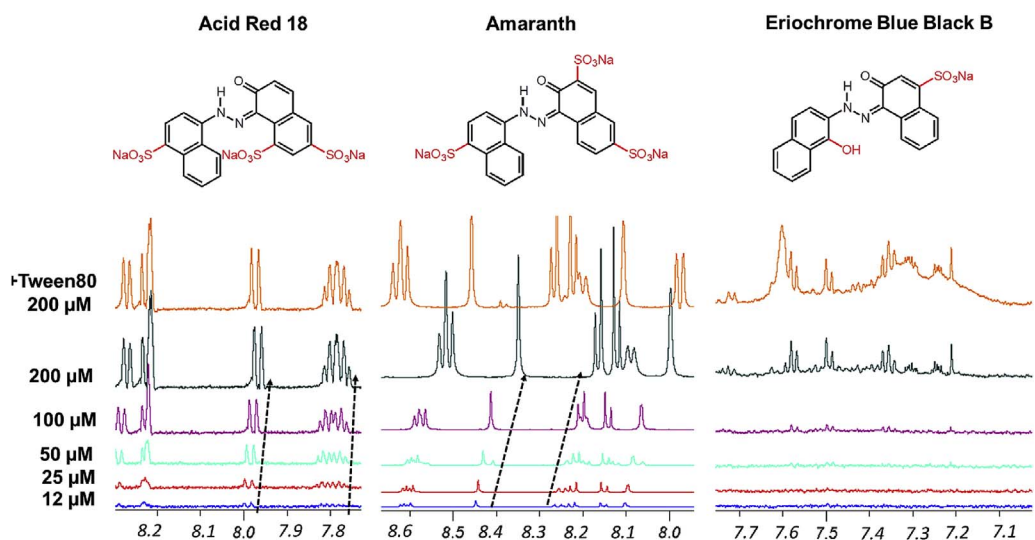


Fig. 8. NMR aggregation assay showing <sup>1</sup>H NMR spectra of three structurally similar bis-naphthyl azo dyes obtained by dilution from 200 μM to 12 μM. Acid red 18 (left), Amaranth (middle), and Eriochrome blue black B (right). (For interpretation of the references to color in this figure legend, the reader is referred to the Web version of this article.)

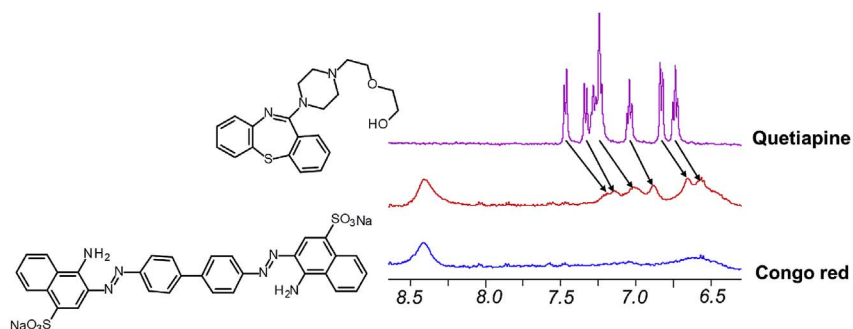


Fig. 9. Shown are NMR spectra of the drug Quetiapine and the dye Congo red. <sup>1</sup>H NMR spectrum of Quetiapine alone (purple above) at 200 μM. <sup>1</sup>H NMR spectrum of 50/50 mixture of Quetiapine and Congo red at 200 μM each (red spectrum, middle) and <sup>1</sup>H NMR of Congo red alone at 200 μM (Blue, bottom spectrum). Note that the broad peaks observed here for free Congo red are less notable in the spectrum of free Congo red in Fig. 3 because the vertical scale is much lower. Samples were prepared in 50 mM sodium phosphate buffer pH 7.4 in 100% D<sub>2</sub>O solvent. (For interpretation of the references to color in this figure legend, the reader is referred to the Web version of this article.)

that minor chemical changes can result in major differences in solution behavior. Our previous work [2], suggested that these solution behaviors can have a serious impact on properties (e.g. toxicity) so it is reasonable that dyes having different behaviors can also have distinct properties. This NMR assay now provides a new tool for monitoring the behavior of dyes in solution, and can begin to explore potential

correlations with relevant properties.

Correlating nano-entities to specific dye properties will certainly prove to be difficult or even impossible. However, it is tempting to hypothesize that aggregate-property relationships can exist. For example, the aggregation property of an HIV drug has been directly attributed to its high and favorable oral bioavailability [16]. Also,

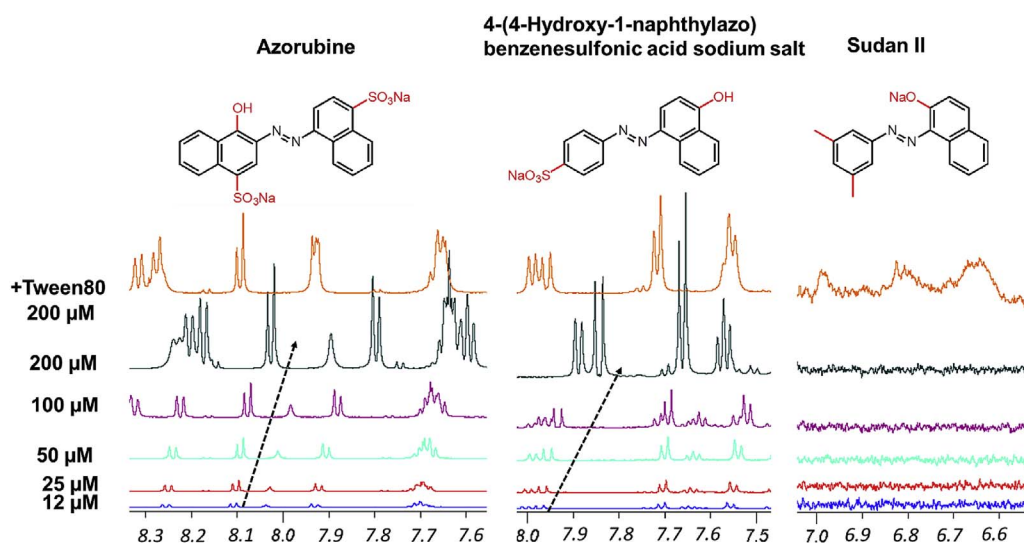


Fig. 10. Portions of the superimposed  $^1\text{H}$  NMR spectra of three structurally similar azo dyes obtained by dilution from  $200\ \mu\text{M}$  to  $12\ \mu\text{M}$ . Azorubine (left), 4-(4-hydroxy-1-naphthylazo)benzenesulfonic acid sodium salt (middle) and Sudan II (right), 1-(2,4-dimethylphenylazo)-2-naphthol. Broken arrows indicate changes in chemical shift ( $\delta$  ppm) with concentration. NMR samples were prepared in  $50\ \text{mM}$  sodium phosphate buffer pH 7.4 in  $100\%$   $\text{D}_2\text{O}$  solvent.

aggregates have been associated with affecting the efficacy of cancer drugs [17,18]. In a 2007 conference in Southampton UK, the use of six dyes (Tartrazine, Sunset Yellow, Allura Red, Acid Red 18, Azorubine and Quinoline Yellow WS) was questioned because they were suspected of causing food intolerance and exasperating attention deficit hyperactivity disorder (ADHD) in children [19]. Interestingly, this study showed that four of the six dyes exhibit nano-entity properties. For example, Azorubine clearly aggregates in our assay as shown in Fig. 10. Other potential properties of dyes are beginning to become evident. For example, some artificial coloring agents appear to aggravate attention deficit hyperactivity disorder (ADHD), and it has been established that erythrosine-based food coloring can cause thyroid tumors in rats. Although little is known about the precise mechanism of toxicity of some dyes, many have been banned (e.g. 42 benzidine and 70 azo dyes) [20].

#### 4. Conclusion

Here we introduced the NMR aggregation assay as a new tool for monitoring the behavior of dyes in solution. One potential utility of this tool is to explore potential correlations with relevant properties. On one hand, we know that dyes have a variety of properties where some are benign and others are toxic and have been banned from human consumption. On the other hand, we also now know that some dyes can have a variety of aggregate behaviors, and aggregates have been shown to exhibit promiscuous properties and even toxicity. Although focused studies will be needed to properly establish behavior-property correlations, the NMR methods shown here may be a good method to provide new insights.

#### Funding

The authors declare no competing financial interest.

#### Acknowledgments

The authors wish to acknowledge Anne-Laure Larroque and Sanjoy Kumar-Das of the McGill University Health Centre (MUHC) for kindly providing 600 MHz NMR time. They also thank Norman Aubry and Rebekah Carson for helpful discussions and insight. Technical support was provided by Sagar Saran and Paul Oguadinma.

#### Appendix A. Supplementary data

Supplementary data related to this article can be found at <http://dx.doi.org/10.1016/j.dyepig.2018.02.026>.

#### References

- [1] LaPlante SR, Aubry N, Bolger G, Bonneau P, Carson R, Coulombe R, et al. Monitoring drug self-aggregation and potential for promiscuity in off-target in vitro pharmacology screens by a practical nmr strategy. *J Med Chem* 2013;56:7073–83. <http://dx.doi.org/10.1021/jm4008714>.
- [2] LaPlante SR, Carson R, Gillard J, Aubry N, Coulombe R, Bordeleau S, et al. Compound aggregation in drug discovery: implementing a practical NMR assay for medicinal chemists. *J Med Chem* 2013;56:5142–50. <http://dx.doi.org/10.1021/jm400535b>.
- [3] Coan KED, Shoichet BK. Stoichiometry and physical chemistry of promiscuous aggregate-based inhibitors. *J Am Chem Soc* 2008;130:9606–12. <http://dx.doi.org/10.1021/ja802977b>.
- [4] <https://chemaxon.com/>.
- [5] McGovern SL, Caselli E, Grigorieff N, Shoichet BK. A common mechanism underlying promiscuous inhibitors from virtual and high-throughput screening. *J Med Chem* 2002;45:1712–22. <http://dx.doi.org/10.1021/jm010533y>.
- [6] Heger D, Jirkovský J, Klán P. Aggregation of methylene blue in frozen aqueous solutions studied by absorption spectroscopy. *J Phys Chem A* 2005;109:6702–9. <http://dx.doi.org/10.1021/jp050439j>.
- [7] Al-Thabaiti SA, Aazam ES, Khan Z, Bashir O. Aggregation of Congo red with surfactants and Ag-nanoparticles in an aqueous solution. *Spectrochim Acta Part A Mol Biomol Spectrosc* 2016;156:28–35. <http://dx.doi.org/10.1016/j.saa.2015.11.015>.
- [8] Zhang Y, Xiang J, Tang Y, Xu G, Yan W. Aggregation behaviour of two thiacyanocyanine dyes in aqueous solution. *Dyes Pigments* 2008;76:88–93.
- [9] Zhegalova NG, He S, Zhou H, Kim DM, Berezin MY. Minimization of self-quenching fluorescence on dyes conjugated to biomolecules with multiple labeling sites via asymmetrically charged NIR fluorophores. *Contrast Media Mol Imaging* 2014;9:355–62. <http://dx.doi.org/10.1002/cmmi.1585>.
- [10] Horowitz VR, Janowitz LA, Modic AL, Heiney PA, Collings PJ. Aggregation behavior and chromonic liquid crystal properties of an anionic monoazo dye. *Phys Rev E - Stat Nonlinear Soft Matter Phys* 2005;72. <http://dx.doi.org/10.1103/PhysRevE.72.041710>.
- [11] Edwards DJ, Jones JW, Lozman O, Ormerod AP, Sintyureva M, Tiddy GJT. Chromonic liquid crystal formation by edicol sunset yellow. *J Phys Chem B* 2008;112:14628–36. <http://dx.doi.org/10.1021/jp802758m>.
- [12] Chami F, Wilson MR. Molecular order in a chromonic liquid crystal: a molecular simulation study of the anionic azo dye sunset yellow. *J Am Chem Soc* 2010;132:7794–802. <http://dx.doi.org/10.1021/ja102468g>.
- [13] Ishiyama M, Shiga M, Sasamoto K, Mizoguchi M, He P. A new sulfonated tetrazolium salt that produces a highly water-soluble formazan dye. *Chem Pharm Bull (Tokyo)* 1993;41:1118–22. <http://dx.doi.org/10.1248/cpb.41.1118>.
- [14] Swerlick RA, Campbell CF. Medication dyes as a source of drug allergy. *J Drugs Dermatol* 2013;12:99–102. <https://www.epa.gov/assessing-and-managing-chemicals-under-tsca/pigment-violet-29-anthra219-def6510-defdiisoquinoline-0>.
- [15] Boutajangout AM, Sigurdsson EK, Krishnamurthy P. Tau as a therapeutic target for Alzheimer's disease. *Curr Alzheimer Res* 2011;8:666–77. <http://dx.doi.org/10.2174/156720511796717195>.
- [16] Frenkel YV, Clark AD, Das K, Wang YH, Lewi PJ, Janssen PAJ, et al. Concentration and pH dependent aggregation of hydrophobic drug molecules and relevance to oral bioavailability. *J Med Chem* 2005;48:1974–83. <http://dx.doi.org/10.1021/jm049439i>.
- [17] Owen SC, Doak AK, Wassam P, Shoichet MS, Shoichet BK. Colloidal aggregation affects the efficacy of anticancer drugs in cell culture. *ACS Chem Biol* 2012;7:1429–35. <http://dx.doi.org/10.1021/cb300189b>.
- [18] <https://www.food.gov.uk/science/additives/foodcolours>.
- [19] <https://www.ncbi.nlm.nih.gov/books/NBK304402/>.

## 2.3 SUPPORTING INFORMATION

The NMR aggregation was employed to other dyes and the displays of the NMR data are shown below as Figures S1 and S2.

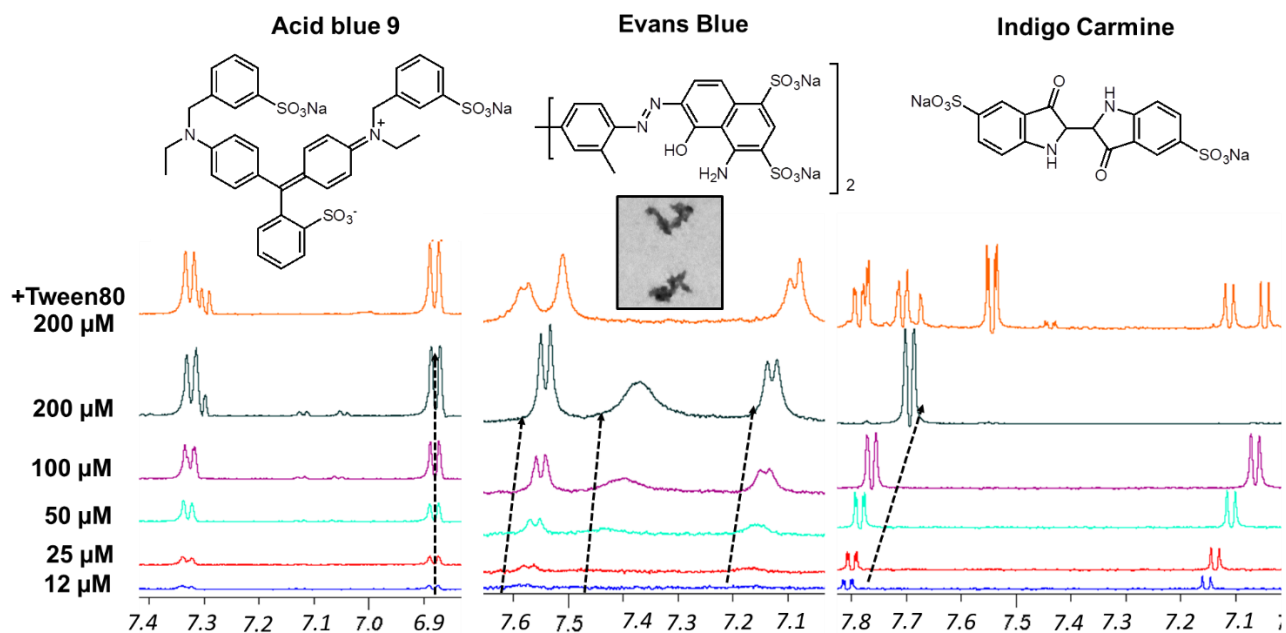


**Figure S1.** Portions of the superimposed <sup>1</sup>H NMR spectra of three structurally different dyes obtained by dilution from 200 μM to 12 μM. Acid blue 9 (left), Evans blue (middle), both medium-sized and Indigo carmine (right). Broken arrows indicate changes in chemical shift (δ ppm) with concentration. NMR samples were prepared in 50 mM sodium phosphate buffer pH 7.4 in 100% D<sub>2</sub>O solvent.

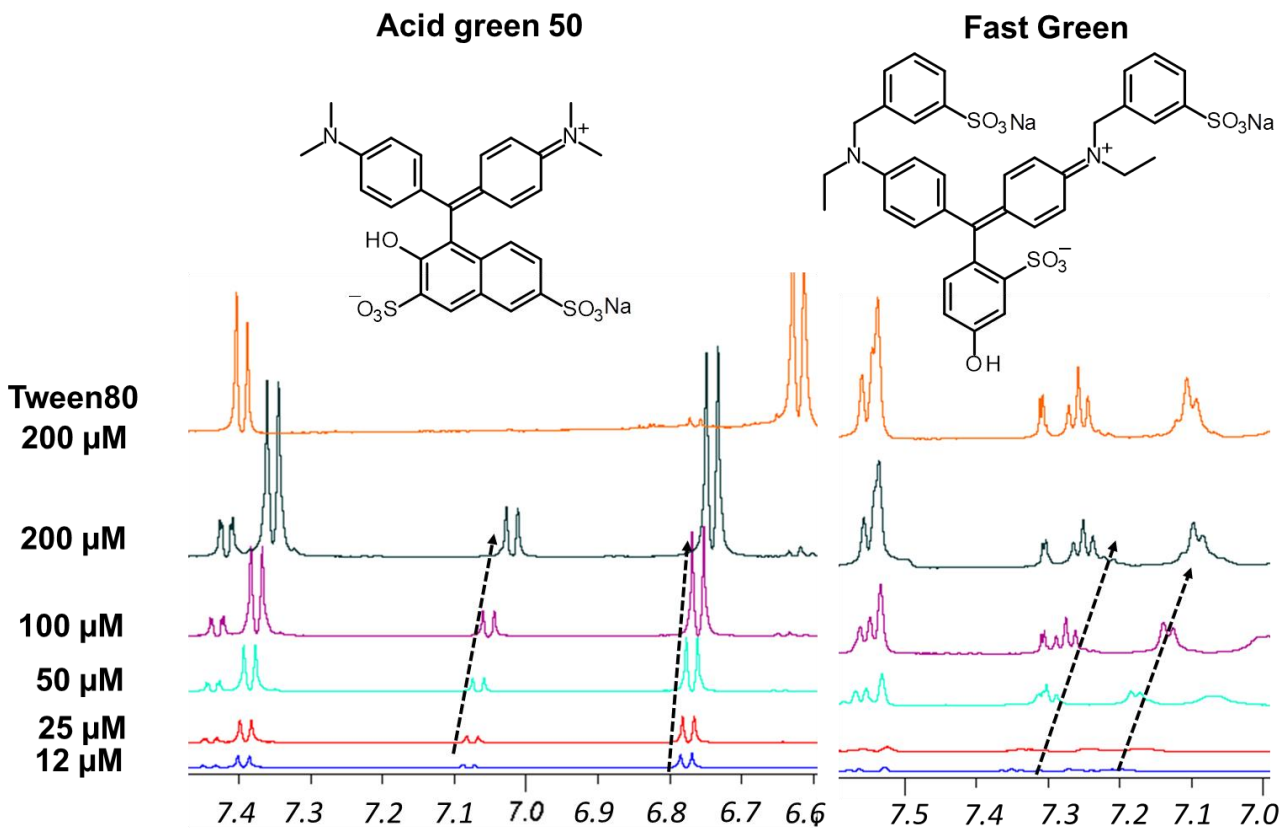


**Figure S2.** Portions of the superimposed  $^1\text{H}$  NMR spectra of Acid Green 50 (left) and Fast Green (right) dyes obtained by dilution from 200  $\mu\text{M}$  to 12  $\mu\text{M}$ . Broken arrows indicate changes in chemical shift ( $\delta$  ppm) with concentration. NMR samples were prepared in 50 mM sodium phosphate buffer pH 7.4 in 100%  $\text{D}_2\text{O}$  solvent.

**CHAPTER 3: SCIENTIFIC ARTICLE (TO BE SUBMITTED)**

**3.1 Contributions of the authors:** A significant portion of this work was carried out by M.D. and F.S., as they contributed equally in terms of design the experiments, sample preparation, cell culture and data acquisition with assistance from M.K. M.D. also helped write the manuscript. S.L. contributed the hypotheses/concepts of the manuscript, supervised the research, interpreted data and helped write the manuscript. P.L. performed some data analysis with input from all authors.

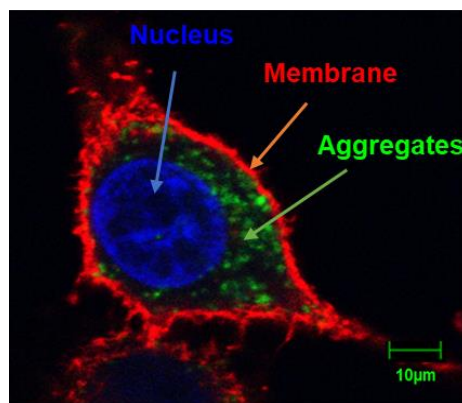
## Revealing Drug Nano-entities

Marwa Dlim,<sup>1,2</sup> Fatma Shahout,<sup>1,2</sup> Marwa Khabir,<sup>1</sup> Patrick Labonte,<sup>1</sup> Steven R. LaPlante<sup>1\*</sup>

<sup>1</sup> Institut National de la Recherche Scientifique, Center Institut Armand-Frappier, Université du Québec, CANADA

<sup>2</sup> These scientists contributed equally to this work and are regarded as both being first authors.

**ABSTRACT:** A compound's aqueous properties are certainly influenced by the nature of its unique equilibria between single lone-tumbling molecules, self-associated aggregates (nano-entities) and solid forms. It is therefore surprising that there is yet no comprehensive and effective strategy for correlating a compound's properties with its physicochemical and nano-entity behavior in solution. Perhaps a better understanding of the equilibria can provide



some insight into unexpected properties of many drugs when placed in aqueous conditions. Here, we use several anticancer drugs (Sorafenib, Lapatinib, Gefitinib and Fulvestrant) and an antileprosy drug (Clofazimine) as model systems to better understand their physicochemical behavior and self-association properties. We explore various techniques modeling a combination of NMR, DLS, electron and confocal microscopies to probe their three-state equilibria and behaviors in buffers, media and cells. These drugs were found to self-associate into relatively large nano-entities having distinct types and sizes that depend on the media. Furthermore, these compounds were capable of entering cells. Noteworthy advantages and “blind spots” were

observed for the various detection techniques employed. Overall, we found that a combination of methods is necessary to expose these drugs' elusive solution equilibria.

The drug discovery community has recognized that the physicochemical attributes of compounds can somehow predispose them to many properties.<sup>1-9</sup> However, the majority of pharma workflows focus on prioritizing compound candidates that exhibit selected favorable properties, and deprioritizing those that have specific undesirable properties, without extensively characterizing their three-state equilibria and associated physicochemical attributes of candidate drugs in aqueous solution. It is becoming more apparent that each compound exists in a unique three-phase equilibrium between single lone-tumbling molecules, self-associated aggregates (nano-entities), and solid forms. Notably, the equilibria and nano-entity attributes and properties vary depending on media which contributes to rich and varied natural phenomenon but also complicates characterization efforts. Thus, it is both interesting and perplexing that the three-state equilibria, and related properties, remain relatively unexplored.

The importance of having insight into a compound's three-state equilibrium can, for example, help predict its tendency to be promiscuous and likelihood of toxicity.<sup>10</sup> These latter properties represent one of the most significant challenges in drug discovery - to date we are still unable to foresee whether or not a medicament will be safe for human consumption despite highly sophisticated rational design efforts.<sup>8, 11-18</sup> Nonetheless, important advances have been made in establishing a qualitative correlation between some physicochemical attributes of toxicity outcomes.<sup>10</sup> It has become common knowledge that although high lipophilicity of drug candidates can serve to improve potency, it also increases its likelihood of resulting in adverse *in vivo* toxicology outcomes. Thus, drug design efforts must qualitatively consider a compound's physicochemical properties, and therefore strive to find a fine balance with regards to the impact of lipophilicity. To do so, a simplistic state-of-the-art tool employed by medicinal chemists is to follow a set of probabilistic guidelines based on an evaluation of a compound's physicochemical attributes from calculated partition coefficient (cLogP) and total polar surface area (TPSA).<sup>11, 19</sup>

Certainly, a more evolved view of a compound's physicochemical properties is wanting, along with improved experimental strategies, to better understand how a compound's physicochemical properties can influence and predispose it to salient properties such as off-target outcomes. To begin, a simplistic view could be that more lipophilic compounds tend to be more

promiscuous by their attraction to hydrophobic off-target receptors.<sup>7</sup> Simply stated, “stickier” compounds can bind non-specifically to “sticky” hydrophobic receptor pockets either in a stoichiometric mode of off-target inhibition (1:1 ligand to target molecule) or nonstoichiometrically ( $\gg$ 1:1 ligands to target). This “sticky” attribute can also contribute to a compound’s tendency to self-associate in aqueous solution into aggregates, also referred to as colloids or nano-entities. However, lipophilicity alone does not explain the nature of a compound’s three-state equilibrium and related properties.<sup>10</sup>

In fact, little is known about the types and range of sizes of self-assemblies that small molecules can adopt, although micelle-like colloids have been reported and recently much smaller nano-entities have also been observed.<sup>10, 20</sup> It is likely that a wide range of sizes and types exist, but detection strategies are lacking and must be developed, which explains in part our poor knowledge of this phenomenon and elusive properties.<sup>21-26</sup> However, progress is being made to reveal some properties which have been implicated, for example, in promiscuity in high-throughput screens (false positives),<sup>21-23</sup> false negatives in cell culture assays due to lack of cell membrane permeability,<sup>27</sup> correlation with off target pharmacology<sup>10</sup> and as having exceptional oral bioavailability.<sup>28, 29</sup>

To date, no single technology can detect the full range of nano-entities that can exist, but each technology has its advantages and limitations. For example, dynamics light scattering (DLS) and transmission electron microscopy (TEM) are sensitive to large homogeneous assemblies (e.g. nanometer size) but are less optimal for small entities and mixtures. NMR spectroscopy, on the other hand, is highly sensitive to small- to medium-sized aggregates (Ångstrom to sub-nanometer sizes). This technology can also be used to detect large aggregates although it requires breaking the aggregates into smaller entities using detergents for detection purposes. Also, confocal laser scanning microscopy (CLSM) can be employed to monitor drugs in cells, but the compounds must be fluorescent and forms sufficiently large assemblies (greater than nanometer sizes). Other potential detection methods can also be used such as nephelometry, SPR, MST, DOSY NMR and CPMG NMR.

Here, we use several anticancer drugs (Sorafenib, Lapatinib, Gefitinib and Fulvestrant) and an antileprosy drug (Clofazimine) as model systems to explore various techniques for monitoring their physicochemical solution behavior. We evaluate data from NMR, DLS, TEM

and CLSM to characterize the nano-entities formed and to probe the strengths and limitations of the methods. It should be kept in mind that the present study focuses on compounds that only form the large micelle-type aggregates. Studies involving the smaller nano-forms are referred to an early report and to forthcoming disclosures.<sup>10, 20</sup>

## RESULTS AND DISCUSSION

A typical workflow practiced in the pharmaceutical industry is one where medicinal chemists synthesize new compounds based on design concepts intended to capture a range of intended favorable properties, e.g. binding and specificity for a target protein, bioavailability, stability and safety. Medicinal chemists almost exclusively characterize their candidate drugs in organic solvents, then lyophilize and expedite the powders or stock solutions to multiple other laboratories for a broad range of pharmaceutical tests where the compounds are dissolved in or diluted with aqueous media. However, drugs behave much differently in organic solvents as compared to aqueous media, and thus the above workflow introduces an important and uncharacterized disconnect. That is, no one along the workflow is responsible for monitoring a compound's aqueous behavior in solution – thus, the three-phase equilibrium systematically goes unexplored.

This is unfortunate because a simple and quick perusal of the <sup>1</sup>H NMR spectrum of a compound in buffer can easily begin to expose features of its three-state equilibrium.<sup>20</sup> This is illustrated in [Figure 1](#) for the four compounds (Sorafenib, Lapatinib, Gefitinib and Clofazimine). These compounds were first placed in organic DMSO-d<sub>6</sub> solvent at 200 μM concentration where it was noted that they dissolved well - clear solutions with no observable precipitate. These stock samples were then transferred to NMR tubes and <sup>1</sup>H NMR spectra acquired, respectively, as shown in [Figure 1a](#). This atomic view of hydrogen nuclei shows that all resonances are observable and sharp, as expected for compounds that behave as single lone-tumbling molecules in solution.

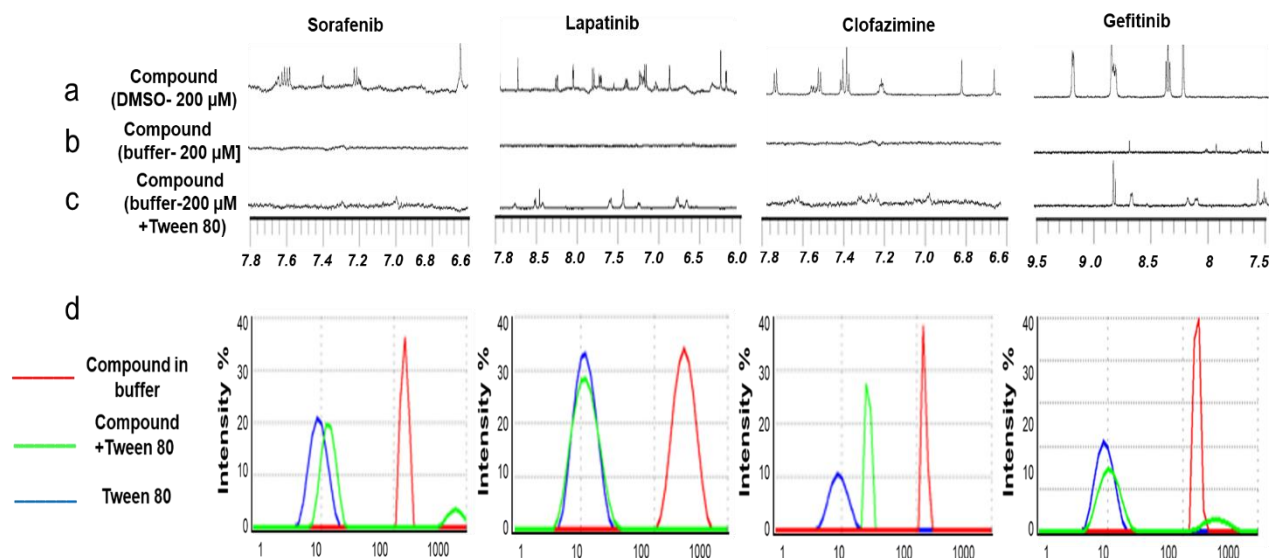


**Figure 1.** NMR spectra of four compounds. (a) Compounds in DMSO- $d_6$  solvent at 20 mM concentration, (b) Compounds in buffer at 20 mM (after mild centrifugation. Then collection of the supernatant) (c) Compounds plus Tween 80 detergent, (d) DLS data of the four compounds employed was in 50 mM sodium phosphate buffer, 100 mM NaCl, 10% D $_2$ O, pH 7.4 in the absence and presence of 0.025% Tween 80 at 24 hrs. Size measured after 24 hrs incubation by DLS (ranged from 200 nm-500 nm).

Samples of these compounds at 200  $\mu\text{M}$  in aqueous buffer were then prepared by placing aliquots of DMSO- $d_6$  stock solutions into aqueous buffer followed by gentle agitation. Some cloudiness or solid precipitate were noted so the samples were subjected to light centrifugation. The supernatant was then placed in NMR tubes and  $^1\text{H}$  NMR spectra acquired. Figure 1b shows that no NMR resonances were observed. It is possible that the compounds totally existed as a solid-state form and were removed by this latter manipulation. Even if some solid remained as a cloudiness, the resonances of solids are too broad to be observed by solution NMR. Another possible explanation would be that the compounds partitioned between precipitates and very large self-associated and soluble aggregates. The latter would have to tumble too slowly in solution which would also result in resonances that are too broad to be observed by solution NMR. Interestingly, we showed in a previous report that a simple trick of adding a detergent such as Triton or Tween to the samples induced the breakup of the large aggregates, resulting in faster tumbling lone molecules, which then gave rise to observable NMR resonances. To our surprise, the addition of detergent to the Sorafenib sample did not give rise to sharp resonances (see Figure 1c), whereas sharp resonances did arise for Lapatinib, Clofazimine and Gefitinib (see Figure 1c).

The latter observations unequivocally report the existence of the large aggregates. However, the lack of resonances for Sorafenib demonstrates our limited knowledge of aggregate types and how to manipulate and observe them by NMR. Interestingly, DLS data acquired on the aqueous samples, after light centrifugation, clearly showed existence of the nanometer sized aggregates (see [Figure 1d](#)). The DLS data of these samples after the subsequent addition of detergent report differential changes in aggregate sizes, which demonstrated the potential complementarity of NMR and DLS techniques.

TEM also convincingly revealed the presence of very large aggregates in various media such as DMEM with 5% fetal bovine serum (FBS) (see [Figure 2a](#)), cell culture media (DMEM) without (FBS) (see [Figure 2b](#)), and aqueous phosphate buffer (see [Figure 2c](#)). First, it must be kept in mind that the samples were prepared by soaking the samples with a carbon-coated copper grid which is required for TEM observation purposes. Also, it is expected that lone-tumbling single molecules (tumbling radius on the single digit Ångstrom scale) would be invisible by TEM which is sensitive to species that have radii on the double digit nanometer scale. Keeping these considerations in mind, a number of observations can nonetheless be made for characterizing these intriguing and large nano-entities observed (see [Figure 2](#)).

Interestingly, a comparison of the horizontal images ([Figure 2c](#)) shows a variety of large aggregates for the drugs in buffer. Some are smaller such as that found for Clofazimine whereas very large globs are noted for Fulvestrant, Sorafenib and Lapatinib. A range of sizes is also noted. Gefitinib appears as a solid-like form. Changes in the aggregates are notable when the compounds are soaked in DMEM media – compare [Figure 2a](#) with [2b](#). Likewise, dramatic changes are observed when comparing all three media conditions (see [Figures 2a, 2b and 2c](#)).

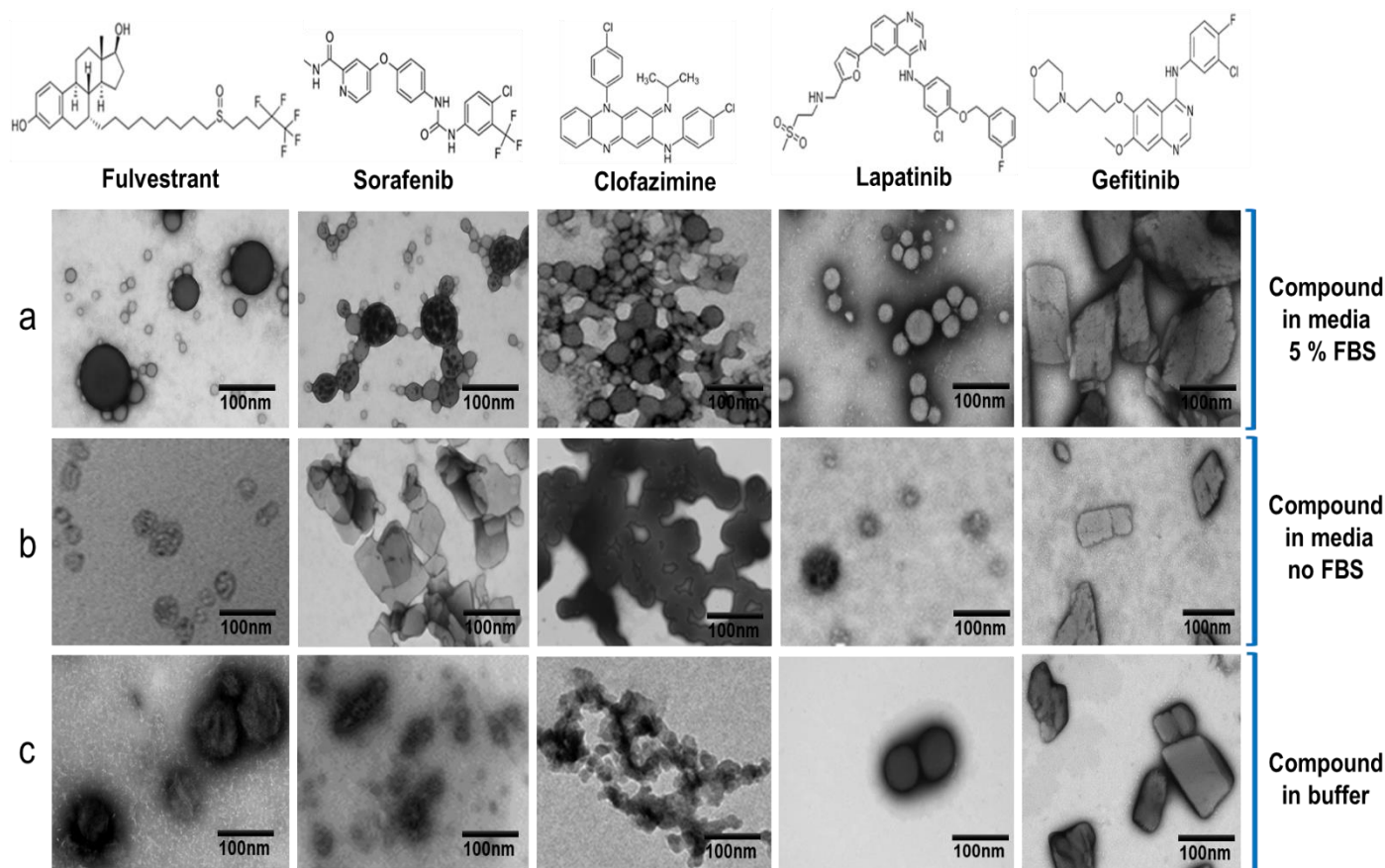


**Figure 2.** TEM images of four aggregating anti-cancer drugs (Sorafenib, Lapatinib, Gefitinib, Fulvestrant), and an aggregating anti-leprosy drug (Clofazimine), (a) Approximately 50  $\mu\text{M}$  of the specified compounds were dissolved and individually incubated for 24 hrs in DMEM 5% FBS, or (b) DMEM with no 5% FBS, or (c) phosphate buffer with pH 7.4. Bars represent 100 nm. We tested another compounds in phosphate buffer and cell culture media as well as the controls as shown in the [Figures S1 and S2](#) in the Supporting Information). DMEM contains a phenol red, glucose, L-glutamine, fetal bovine serum (FBS) and penicillin antibiotic.

We then studied the effect of adding detergent to large nano-entities. The addition of detergents to samples suspected of forming large aggregates is a widely used strategy in many biochemical assays to reveal false positive hits in screening campaigns. One typically runs screening campaigns to identify lone-tumbling compounds that inhibit a protein, but these assays are frequently contaminated with false-positive hits from compounds that form large aggregates that inhibit via non-stoichiometric and non-specific means. Running follow-up validation screens

typically involves the addition of a detergent, which presumably breaks up drug aggregates, and results in the loss of false-positive inhibition.

We thus explored the effect of the addition of detergents on the aggregates of the drugs studied here (see Figure 3a). The TEM images shown in Figure 3a for Sorafenib, Lapatinib and Clofazimine (in the absence of detergent) clearly display large aggregates. Upon addition of 0.025% Tween 80 detergent, the TEM images in Figure 3b show that these large aggregates are seriously altered and disrupted. Taking the  $^1\text{H}$  NMR experiments in Figure 1 into account, it is clear that addition of detergent breaks the aggregates into very small tumbling entities for Lapatinib and Clofazimine, which is consistent with the TEM changes in Figure 3b. However, small entities were not observed for Sorafenib upon addition of detergent whereas the TEM data clearly shows disruption of the large aggregates. Therefore, the example of Sorafenib demonstrates that there might be aggregate types that NMR and TEM simply cannot detect.

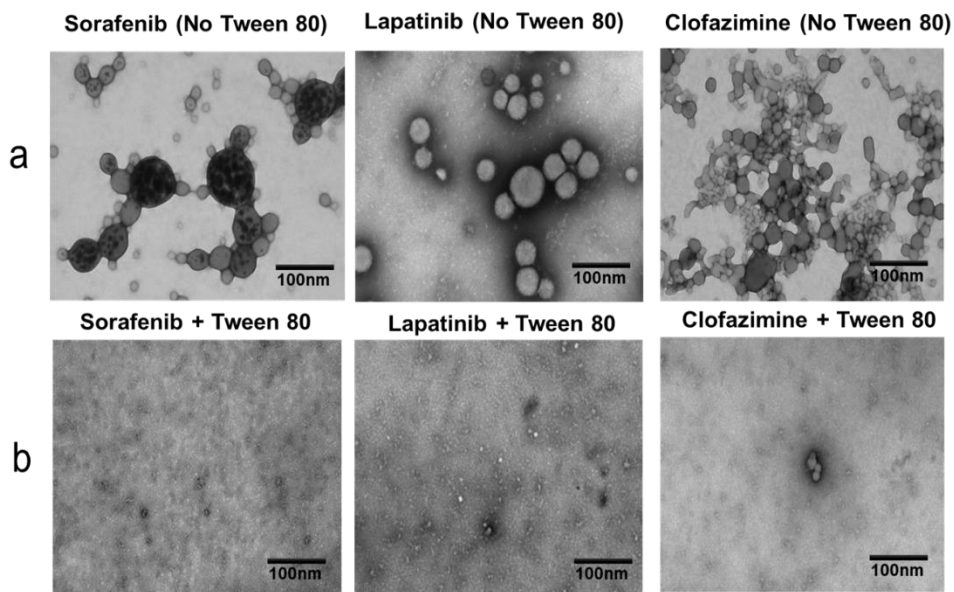


**Figure 3.** (a) TEM images of 50  $\mu\text{M}$  Sorafenib, Lapatinib and Clofazimine, after incubation for 24 hrs at 37  $^{\circ}\text{C}$  in DMEM 5% FBS in the absence of 0.025% Tween 80. (b) TEM images of these compounds in the presence of Tween 80. Bar represent 100 nm.

The subfield of drug self-assemblies has always been full of assumptions and dogma. Two notable contention assumptions are that compound aggregates cannot exist in plasma nor be able

to cross membranes to enter cells.<sup>30</sup> The former assumption has often been rationalized based on the observations that typical drug compounds are formed to be highly serum-bound *in vivo*<sup>31</sup> low free-state concentrations. Given this, the majority of a compound would be expected to be bound to serum proteins such as albumin, leaving compounds mostly unavailable to self-associate. This assumption is unfounded. In a previous study, involving an NMR aggregation test, it was clearly shown that aggregating compounds remained self-associated in a range of pharmacology buffers, plasma and blood. This would suggest that there is a significant affinity for self-association for some compounds.<sup>10</sup>

Regarding the latter assumption, we set out here to identify tools that can help determine if aggregating compounds can cross membranes and enter cells. For this, we explored the use of confocal laser scanning microscopy (CLSM). First, one must realize and consider that all the methods used here make observations at very distinct resolutions. NMR makes measurements at the atomic level or Ångstroms, whereas TEM and DLS resolve particles at the nanometer scale, and CLSM at the micrometer level. Thus, CLSM is the most appropriate method for observations at the cellular level. However, to render a compound observable by CLSM, it must inherent fluorescence, so we were limited in the compounds that could be studied – so potential compounds were pre-screened by a standard fluorescent microscope.

We began this study by the incubation of HeLa cells in the presence of Lapatinib at 50  $\mu$ M for 24 hours and acquired CLSM views (see [Figure 4a](#)). Views from a range of other concentrations, conditions and compounds are provided in the Supporting Information, along with a description of the procedures employed and experimental information. [Figure 4a](#) shows that the green fluorescent of Lapatinib indeed had entered the cell and appears mostly localized to the cytoplasm. Note that the cell membrane and nuclei can be visualized (see [Figure 4a](#)) based on the red and blue dyes Alexa Fluor® 555 conjugate of WGA and DRAQ5™, respectively, which are well-known markers. Interestingly, Lapatinib appears to be well-distributed within the cytoplasm given that green fluorescence is observed for all the cytoplasm.

This is certainly distinct from the observations for Clofazimine. Clofazimine was incubated with Huh-7 cells for 1 hour (see [Figure 4b](#)) (a range of other concentrations, conditions were also tested and are shown in the Supporting Information [Figure S8](#)). Although [Figure 4b](#) shows a well-distributed green fluorescence within the cytoplasm, there are strong compound

signals arising from the nucleus. Note that the nuclei can be visualized (see Figure 4b) based on the blue dye DAPI, but the cell membrane cannot be easily distinguish given that no Alexa Fluor® 555 conjugate of WGA dye was added in this experiment due to signal interferences. In order to verify that the compound aggregates were occurring intra- and not extra-cellularly, care was taken to wash the cells after the incubation step. They were washed twice in phosphate-buffered saline (PBS) to remove any existing extracellular aggregates, and fresh DMEM 5% FBS were added to the cells.

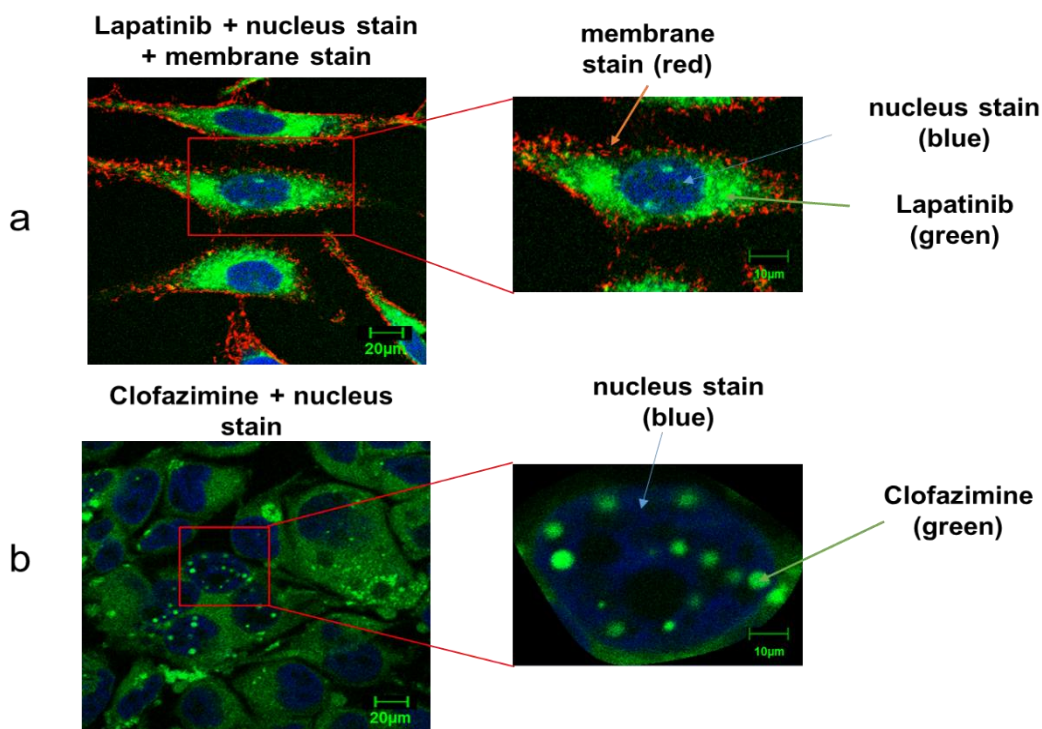


**Figure 4.** (a) Confocal images of HeLa cells incubated in the presence of 50  $\mu\text{M}$  Lapatinib aggregates for 24 hrs at 37  $^{\circ}\text{C}$ , Alexa fluor WGA 555 was used to stain and indicate cell membranes, DRAQ5<sup>TM</sup> was used to stain the nucleus. Bar represents 20  $\mu\text{m}$ . (b) CLSM images of Huh-7 cells incubated in the presence of 20  $\mu\text{M}$  Clofazimine treatment for 1 hr at 37  $^{\circ}\text{C}$  fluorescence of intracellular Clofazimine aggregates. DAPI was used to stain the nucleus. Bar represents 20  $\mu\text{m}$ .

It is interesting that Clofazimine is considered as a lipophilic antibiotic which has very long pharmacokinetic half-life reach up to 70 days.<sup>32</sup> Others have noted that Clofazimine aggregates/accumulates in cells (*in vitro*) over several days, where it was noted that they form

intracellular inclusions in the cytoplasm. It was also reported that Clofazimine can be toxic as it induces changes to the mitochondria structure and function.<sup>32</sup>

Our study also employed ultra-thin section electron microscopy (USEM), as a complementary technique with higher resolution at the nanometer scale, to observe aggregates within cells. The USEM images involving Clofazimine, Lapatinib and Light green SF Yellowish (see [Figure S9](#) in the Supporting Information). Interestingly, they also appeared to resemble the size, number and distribution to the drugs inclusions observed by transmission light microscopy.

## CONCLUSION

This work begins the process of evaluating available tools for detecting large nano-entities. We found some strengths and weaknesses of a set of techniques, which nonetheless together have allowed us to reveal features of nano-entities from the atomic level to the micrometer scale. It was noted that these large nano-entities can adopt a variety of sizes and types that highly depend on the solution conditions. It was also confirmed that compounds that form nano-entities can indeed enter cells and have properties.

It is apparent that the two-state model (lone tumbling molecules and solids form) for describing compound behavior in aqueous solution must be expanded to include soluble aggregates – hence the three-state model. It is our assessment that the scientific community has only begun to reveal this fascinating nano-world. First, a platform of techniques needs to be established, which will allow the scientific community to characterize nano-entities then establish their correlation with salient properties. For example, it has already been established that large-nano-entities can be correlated with compounds high bioavailability, promiscuity, false-positives in screens, etc. Perhaps a better understanding of nano-entities can help minimize drug side-effect, promote safer compounds to the clinic, or to serve as drug delivery systems. For example, the corresponding author has used the detection of aggregates to deprioritize promiscuous drug candidates and promote selective compounds for the clinic.<sup>20, 33, 34</sup>

## ASSOCIATED CONTENT

### Supporting Information

Experimental methods, supplemental figures and tables, and associated references ([PDF](#))

## AUTHOR INFORMATION

### Corresponding Authors

Email: [Steven.LaPlante@iaf.inrs.ca](mailto:Steven.LaPlante@iaf.inrs.ca)

### Author Contributions

A significant portion of this work was carried out by M.D. and F.S., as they contributed equally in terms of design the experiments, sample preparation, cell culture and data acquisition with assistance from M.K. M.D. also helped write the manuscript. S.L. contributed the hypotheses/concepts of the manuscript, supervised the research, interpreted data and helped write the manuscript. P.L. performed some data analysis with input from all authors.

## ACKNOWLEDGMENTS

The authors wish to acknowledge the members of technicians in the INRS institute; Jessy Tremblay for his help in Confocal Microscopy, Micheline Letarte and Arnaldo Nakamura for in transmission electron micrograph analysis. This work was supported by the Libyan Government, NSERC CRCNG, and NMX.

## REFERENCES

1. Leeson, P. D., and Springthorpe, B. (2007) The influence of drug-like concepts on decision-making in medicinal chemistry, *Nat. Rev. Drug Discov.* 6, 881.
2. Lipinski, C. A., Lombardo, F., Dominy, B. W., and Feeney, P. J. (1997) Experimental and computational approaches to estimate solubility and permeability in drug discovery and development settings, *Adv. Drug Del. Rev.* 23, 3-25.
3. Lipinski, C. A. (2004) Lead-and drug-like compounds: the rule-of-five revolution, *Drug Discovery Today: Technologies* 1, 337-341.
4. Vieth, M., Siegel, M. G., Higgs, R. E., Watson, I. A., Robertson, D. H., Savin, K. A., Durst, G. L., and Hipskind, P. A. (2004) Characteristic physical properties and structural fragments of marketed oral drugs, *J. Med. Chem.* 47, 224-232.
5. Proudfoot, J. R. (2005) The evolution of synthetic oral drug properties, *Bioorg. Med. Chem. Lett.* 15, 1087-1090.
6. Morphy, R. (2006) The influence of target family and functional activity on the physicochemical properties of pre-clinical compounds, *J. Med. Chem.* 49, 2969-2978.
7. Van De Waterbeemd, H., Smith, D. A., Beaumont, K., and Walker, D. K. (2001) Property-based design: optimization of drug absorption and pharmacokinetics, *J. Med. Chem.* 44, 1313-1333.
8. Cronin, D., and Mark, T. (2006) The role of hydrophobicity in toxicity prediction, *Curr. Comput. Aided Drug Des.* 2, 405-413.
9. Meanwell, N. A. (2011) Improving drug candidates by design: a focus on physicochemical properties as a means of improving compound disposition and safety, *Chem. Res. Toxicol.* 24, 1420-1456.
10. LaPlante, S. R., Aubry, N., Bolger, G., Bonneau, P., Carson, R., Coulombe, R., Sturino, C., and Beaulieu, P. L. (2013) Monitoring drug self-aggregation and potential for promiscuity in off-target in vitro pharmacology screens by a practical NMR strategy, *J. Med. Chem.* 56, 7073-7083.
11. Price, D. A., Blagg, J., Jones, L., Greene, N., and Wager, T. (2009) Physicochemical drug properties associated with in vivo toxicological outcomes: a review, *Expert Opin. Drug Metab. Toxicol.* 5, 921-931.
12. Kola, I., and Landis, J. (2004) Can the pharmaceutical industry reduce attrition rates?, *Nature reviews Drug discovery* 3, 711.

13. Blagg, J. (2006) Structure–activity relationships for in vitro and in vivo toxicity, *Annu. Rep. Med. Chem.* 41, 353-368.
14. Kramer, J. A., Sagartz, J. E., and Morris, D. L. (2007) The application of discovery toxicology and pathology towards the design of safer pharmaceutical lead candidates, *Nature Reviews Drug Discovery* 6, 636.
15. Azzaoui, K., Hamon, J., Faller, B., Whitebread, S., Jacoby, E., Bender, A., Jenkins, J. L., and Urban, L. (2007) Modeling promiscuity based on in vitro safety pharmacology profiling data, *ChemMedChem* 2, 874-880.
16. Stevens, J. L., and Baker, T. K. (2009) The future of drug safety testing: expanding the view and narrowing the focus, *Drug Discov. Today* 14, 162-167.
17. Krejsa, C. M., Horvath, D., Rogalski, S. L., Penzotti, J. E., Mao, B., Barbosa, F., and Migeon, J. C. (2003) Predicting ADME properties and side effects: the BioPrint approach, *Current Opinion in Drug Discovery and Development* 6, 470-480.
18. Cronin, M. T. (2004) *Predicting chemical toxicity and fate*, CRC press.
19. Hughes, J. D., Blagg, J., Price, D. A., Bailey, S., DeCrescenzo, G. A., Devraj, R. V., Ellsworth, E., Fobian, Y. M., Gibbs, M. E., and Gilles, R. W. (2008) Physiochemical drug properties associated with in vivo toxicological outcomes, *Bioorg. Med. Chem. Lett.* 18, 4872-4875.
20. LaPlante, S. R., Carson, R., Gillard, J., Aubry, N., Coulombe, R., Bordeleau, S., Bonneau, P., Little, M., O'Meara, J., and Beaulieu, P. L. (2013) Compound aggregation in drug discovery: implementing a practical NMR assay for medicinal chemists, *J. Med. Chem.* 56, 5142-5150.
21. Seidler, J., McGovern, S. L., Doman, T. N., and Shoichet, B. K. (2003) Identification and prediction of promiscuous aggregating inhibitors among known drugs, *J. Med. Chem.* 46, 4477-4486.
22. Feng, B. Y., Simeonov, A., Jadhav, A., Babaoglu, K., Inglese, J., Shoichet, B. K., and Austin, C. P. (2007) A high-throughput screen for aggregation-based inhibition in a large compound library, *J. Med. Chem.* 50, 2385-2390.
23. McGovern, S. L., Helfand, B. T., Feng, B., and Shoichet, B. K. (2003) A specific mechanism of nonspecific inhibition, *J. Med. Chem.* 46, 4265-4272.
24. Doak, A. K., Wille, H., Prusiner, S. B., and Shoichet, B. K. (2010) Colloid formation by drugs in simulated intestinal fluid, *J. Med. Chem.* 53, 4259-4265.

25. Coan, K. E., and Shoichet, B. K. (2008) Stoichiometry and physical chemistry of promiscuous aggregate-based inhibitors, *J. Am. Chem. Soc.* *130*, 9606-9612.
26. Wang, J., and Matayoshi, E. (2012) Solubility at the molecular level: development of a critical aggregation concentration (CAC) assay for estimating compound monomer solubility, *Pharm. Res.* *29*, 1745-1754.
27. Owen, S. C., Doak, A. K., Wassam, P., Shoichet, M. S., and Shoichet, B. K. (2012) Colloidal aggregation affects the efficacy of anticancer drugs in cell culture, *ACS Chem. Biol.* *7*, 1429-1435.
28. Frenkel, Y. V., Clark, A. D., Das, K., Wang, Y.-H., Lewi, P. J., Janssen, P. A., and Arnold, E. (2005) Concentration and pH dependent aggregation of hydrophobic drug molecules and relevance to oral bioavailability, *J. Med. Chem.* *48*, 1974-1983.
29. Volovik Frenkel, Y., Gallicchio, E., Das, K., Levy, R. M., and Arnold, E. (2009) Molecular dynamics study of non-nucleoside reverse transcriptase inhibitor 4-[[4-[[4-[(E)-2-cyanoethenyl]-2, 6-dimethylphenyl] amino]-2-pyrimidinyl] amino] benzonitrile (TMC278/rilpivirine) aggregates: correlation between amphiphilic properties of the drug and oral bioavailability, *J. Med. Chem.* *52*, 5896-5905.
30. Ganesh, A. N., Donders, E. N., Shoichet, B. K., and Shoichet, M. S. (2018) Colloidal aggregation: From screening nuisance to formulation nuance, *Nano Today*.
31. Lu, J., Owen, S. C., and Shoichet, M. S. (2011) Stability of self-assembled polymeric micelles in serum, *Macromolecules* *44*, 6002-6008.
32. Baik, J., and Rosania, G. R. (2011) Molecular imaging of intracellular drug–membrane aggregate formation, *Mol. Pharm.* *8*, 1742-1749.
33. Beaulieu, P. L., Bolger, G., Deon, D., Duplessis, M., Fazal, G., Gagnon, A., Garneau, M., LaPlante, S., Stammers, T., and Kukolj, G. (2015) Multi-parameter optimization of aza-follow-ups to BI 207524, a thumb pocket 1 HCV NS5B polymerase inhibitor. Part 2: Impact of lipophilicity on promiscuity and in vivo toxicity, *Bioorg. Med. Chem. Lett.* *25*, 1140-1145.
34. LaPlante, S. R., Bös, M., Brochu, C., Chabot, C., Coulombe, R., Gillard, J. R., Jakalian, A., Poirier, M., Rancourt, J., and Stammers, T. (2013) Conformation-based restrictions and scaffold replacements in the design of hepatitis C virus polymerase inhibitors: discovery of deleobuvir (BI 207127), *J. Med. Chem.* *57*, 1845-1854.

### **3.3 SUPORTING INFORMATION**

#### **Revealing Drug Nano-entities**

**Marwa Dlim<sup>1,2</sup>, Fatma Shahout<sup>1,2</sup>, Marwa Khabir<sup>1</sup>, Patrick Labonte<sup>1</sup>, Steven R. LaPlante<sup>1\*</sup>**

Université du Québec, Institut national de la recherche scientifique  
Center INRS-Institut Armand-Frappier

## **Experimental Methods**

**Compounds (drugs and dyes)** The drugs and dyes used in this study were obtained from commercial vendors. their CAS numbers are as following: Sorafenib (284461-73-0) from Synchem, Inc.; Fulvestrant (129453-61-8) from Sigma; Lapatinib (388082-78-8) from Larid Road; Clofazimine (2030-63-9) from Sigma; Tartrazine (1934-21-0), and Light Green SF Yellowish (5141-20-8) from Alfa Aesar. Alexa fluor WGA555 and Prolong Diamond Anti-fade with DAPI was purchased from Thermo Fisher Scientific.

### **Transmission Electron Micrograph**

The compounds were diluted in 50 mM sodium phosphate pH 7.4 in DMEM 5% FBS. Next, 100  $\mu$ L of the samples were transferred into a 240  $\mu$ L Airfuge tube. A carbon-coated copper grid was inserted into the bottom of the Airfuge tube with fine tweezers and centrifuged for 5 mins at 20 psi. The carbon grid was gently removed with tweezers and washed with distilled water for 1 min. The carbon grid was negatively stained with 3% of phosphotungstic acid (PTA-3) for 1 min. The grid was removed, blotted, dried with a bibulous paper, and examined under a transmission electron microscope (Hitachi H-7100). The photographs were processed with the digital camera AMT version 600.147.

### **Cell Culture**

HeLa and Huh-7 cell lines were maintained in Dulbecco's Modified Eagle's Medium (DMEM) supplemented with 5% of fetal bovine serum albumin (FBS).

### **Confocal Laser Scanning Microscopy (CLSM)**

CLSM was employed to observe the self-aggregation of compounds within the cells. HeLa and Huh-7 cells were grown on glass coverslips in 24 well plates and cultured overnight in DMEM (5% FBS, 1% penicillin/streptomycin) at 37 °C in 5% CO<sub>2</sub>. After removing the culture media and washing them twice with PBS, compounds at the given concentrations were dissolved in DMEM 5% FBS and added to the wells. After 1, 2, 4, 6 and 24 hrs incubation, the cells were washed two times with 1 X PBS and treated with Alexa Fluor WGA555 for membrane staining. The cells were then fixed in 4% paraformaldehyde solution for 10 minutes and washed twice with PBS 1 X. Further, the coverslips were mounted on a prolong diamond antifade with DAPI nucleus staining

for Clofazimine and Light green SF Yellowish and DRAQ-5 for Lapatinib. The cells were imaged by a Zeiss CLSM-780 confocal microscopy (ZEISS, Jena, Germany) on an Olympus FV1000 at 60X magnification, using the following excitation and emission wavelengths: for DAPI, excitation was at 405 nm and emission at 460 nm; for Alexa Fluor WGA555, excitation and emission were at 520 nm and 550 nm, respectively. Excitation and emission at 405 nm and 460 nm, respectively, were employed for the detection of Lapatinib aggregates.

### **Cell Proliferation Assay and *In Vitro* Cytotoxicity Study (MTT Assay)**

The cytotoxicity of the panel of compounds and DMSO were evaluated *in vitro* employing MTT assays. HeLa and Huh-7 cells were plated in 96 well plates and cultured overnight in DMEM 5% FBS, in the absence or presence of compounds. After removing the culture medium, various concentrations of compound were dissolved in DMSO -DMEM 5% FBS, added to the cells, and incubated for 24 hrs. The medium in each well was then aspirated and discarded. Next, 10  $\mu$ L of 5 mg/ml BPS MTT solution, 3-(4,5-dimethylthiazol-2,5-diphenyl tetrazolium bromide), was added to each well and incubated for 2 to 4 hrs. Following incubation, the medium was replaced with 150  $\mu$ L DMSO solution to dissolve the purple crystals. After 15 mins, the optical densities at 570 nm were measured by Spectrophotometer.

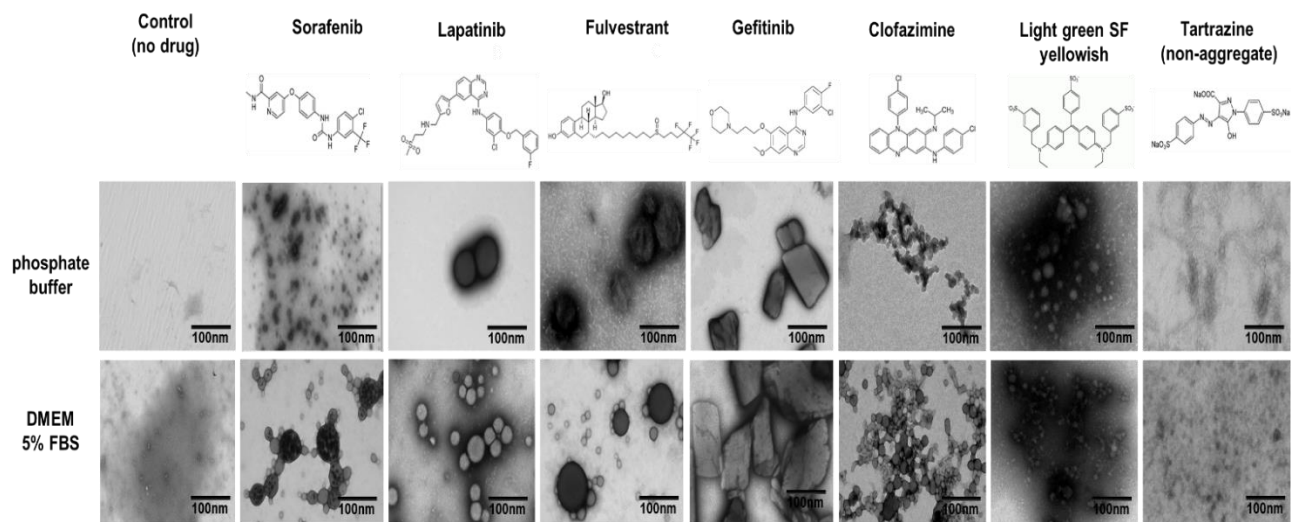
### **Dynamic Light Scattering**

Compounds were dissolved in 1% DMSO and added to the cells at the desired final concentrations. The size of the aggregates was measured in the DMEM 5% FBS or phosphate buffer, pH 7.4. Measurements were performed by polystyrol/polystyrene 10 x 10 x 45 mm cuvettes, utilizing the Zetasizer Nano ZS (Malvern), version 1.7, with a 60 Mw laser operating at 830 nm and a detector angle of 158°. All samples were centrifuged before analysis performed in triplicate at 25 °C and the data were acquired using the Dynamics software. All compounds were at 50  $\mu$ M.

### **Thin-Section Electron Microscopy**

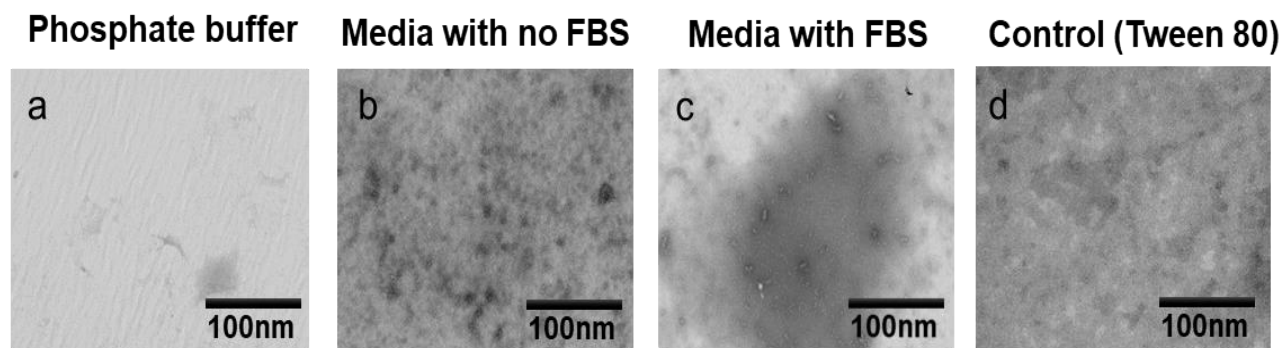
The cells were plated at  $1 \times 10^5$  cells/well and incubated in the presence 50  $\mu$ M of all compounds for 24 hrs. The medium was then aspirated, and the cells washed two times with 1 X PBS. The cells were then fixed with glutaraldehyde (2.5% in 0.1 M cacodylate buffer or phosphate-buffered saline, overnight) and again washed 2X with PBS. Next, the cells were collected and centrifuging at 1000 x g for 10 mins. The fixed cell pellets were re-suspended in a freshly prepared solution

1.3 % (w/v) osmium tetroxide in a colliding buffer for 1-2 hrs and then dehydrated by successive washes with 25, 50, 75 and 95% solutions of acetone in water (15-30 mins each). This was followed by two changes of pure acetone incubated for 30 mins each. The cell pellets were then re-suspended in SPURR acetone (1:1) and incubated for 16-18 hrs at room temperature. The cells were cut into small pieces and placed in BEEM<sup>®</sup> capsules to capacity. The capsules were incubated at 600-650 °C for the polymerization reaction to occur. The final stage involved cutting the embedded cells into ultra-thin sections and placing the sections on a carbon-covered copper 200-mesh grid. The grids were then stained with 50 % ethanol for 20-25 mins. Examination of the sections was performed using an electron microscope (Hitachi H-7100), and the photographs were processed using the digital camera AMT, version 600.147.



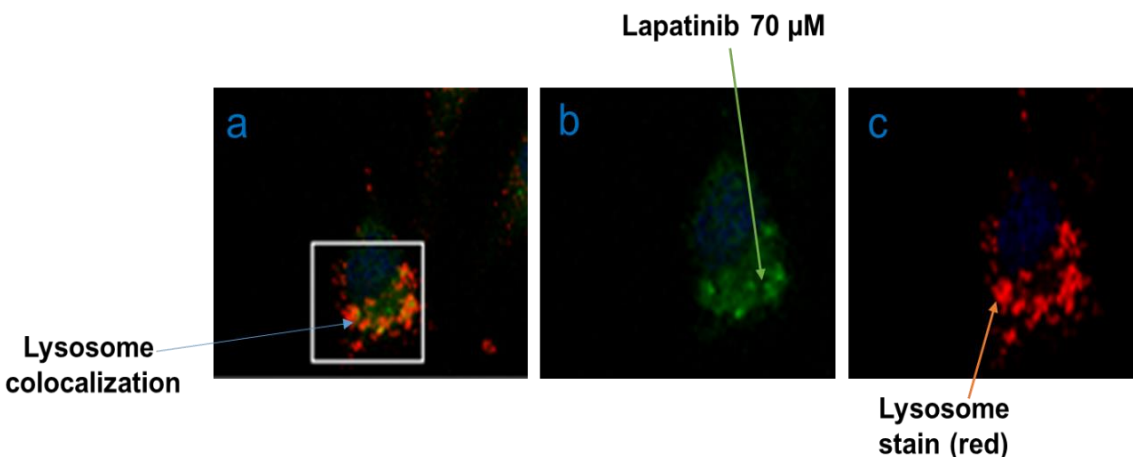
**Figure S1.** TEM images of seven compounds, which includes four aggregating anti-cancer drugs (Sorafenib, Lapatinib, Fulvestrant and Gefitinib), one aggregating anti-leprosy drug (Clofazimine), and two dyes (one aggregating Light Green SF Yellowish and one non-aggregating Tartrazine). Approximately 50  $\mu\text{M}$  of the seven specified compounds were dissolved and individually incubated for 24 hrs in either in 50 mM sodium phosphate, with pH 7.4 (top row) or in DMEM 5% FBS (bottom row). Bars represent 100 nm.

TEM in Figure S1 notable differences in aggregate formation size and shape for each compound. For example, the anti-cancer compounds Sorafenib, Lapatinib, Fulvestarne and antileprosy Clofazimine formed spherical homogenous aggregates which stick to each other, whereas Gefitinib behaved as a large crystal in both phosphate buffer and cell culture media.

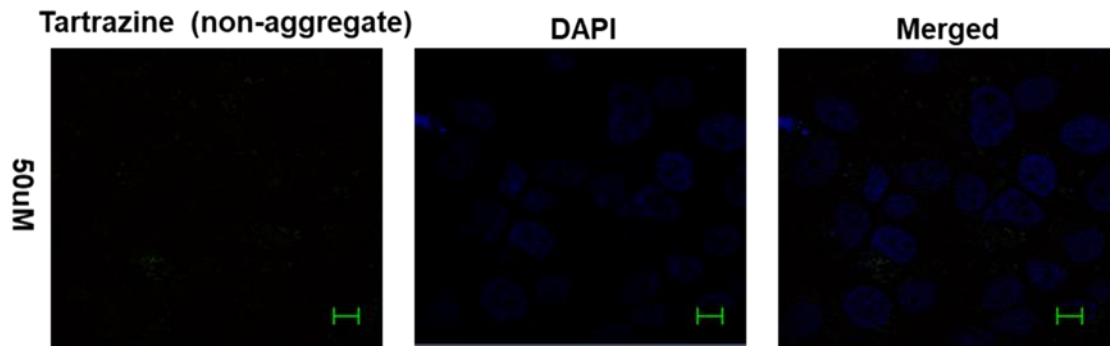


**Figure S2.** TEM images showed the controls where are no drugs, a) phosphate buffer, b) cell culture media with no FBS, c) cell culture media with 5% FBS, d) Tween 80. Bar represent 100 nm.

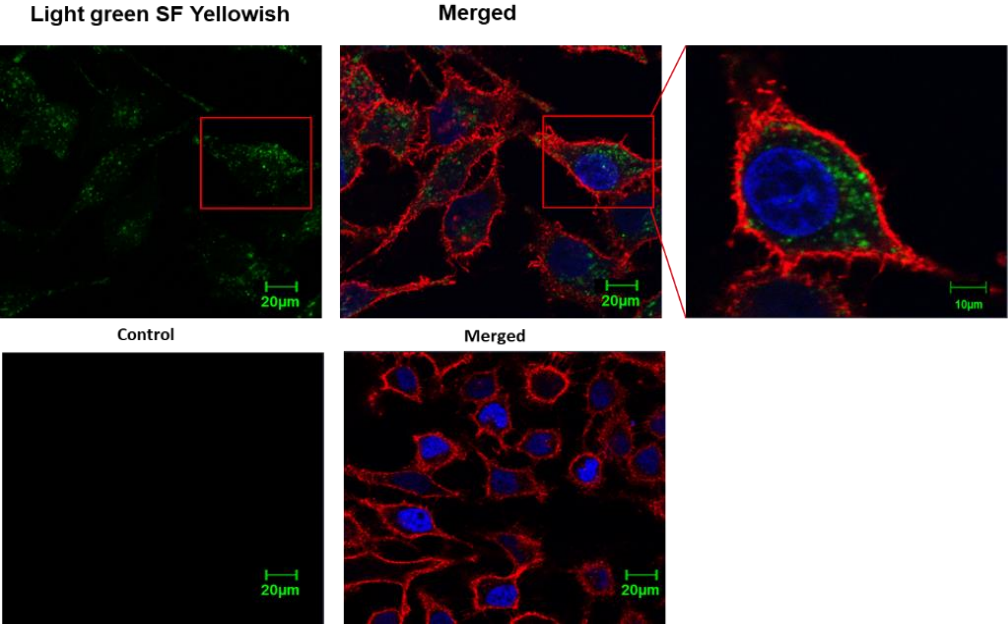
The figure below shown Lapatinib colloids co-localize to endolysosomal compartments, as indicated by fluorescent aggregates (green) with a lysosomal stain marker (lyso-tracker red). In addition, the color change from green to orange which indicates the co-localization and internalization of Lapatinib in the lysosomal compartment.



**Figure S3.** CLSM images of HeLa cells incubated in the presence of 70  $\mu\text{M}$  of Lapatinib. Intracellular aggregates indicate that the nano-entities form within the lysosomal compartments. (a) Merged Lapatinib particles co-localized with the lysosome, (b) Lapatinib aggregates (green), (c) lysotracker (red). The nuclear stain was DRAQ5 (blue). Bars represent 20  $\mu\text{m}$ .

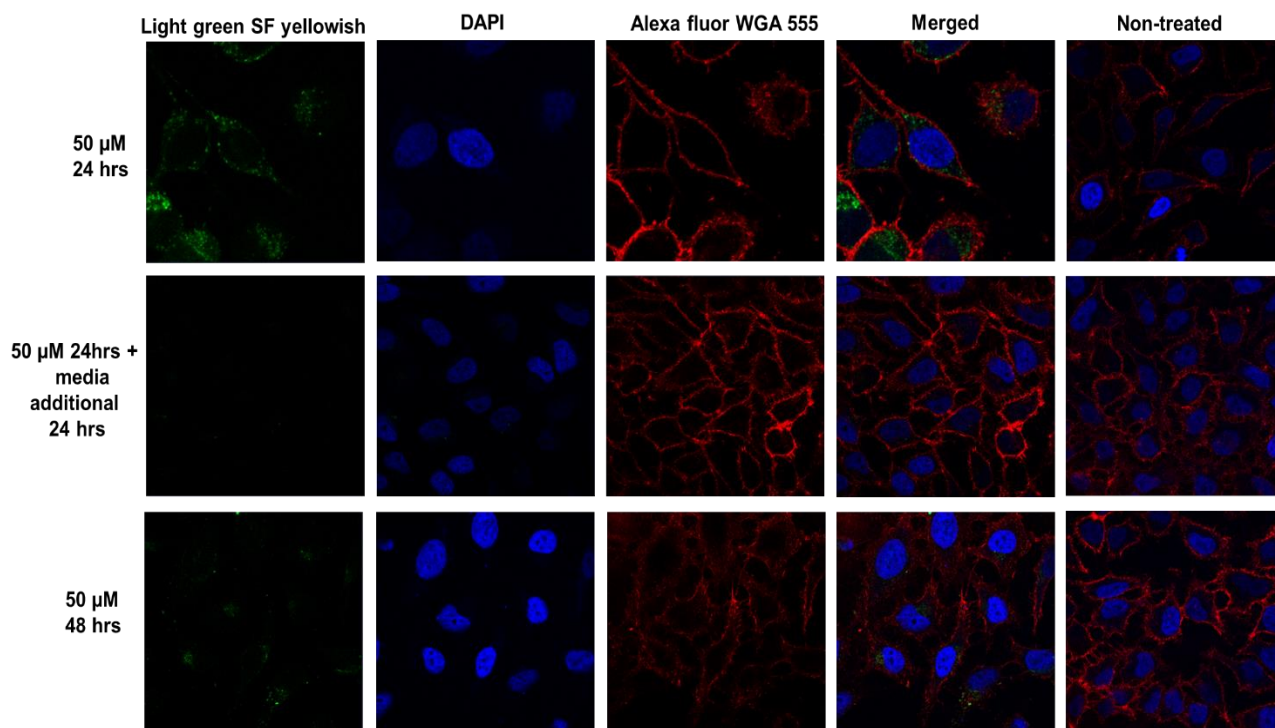


**Figure S4.** Confocal images of Huh-7 cells incubated in the presence of 50  $\mu\text{M}$  of Tartrazine dye (non-aggregator dye) incubated for 24 hrs at 37  $^{\circ}\text{C}$ . Bars represent 100  $\mu\text{m}$ .

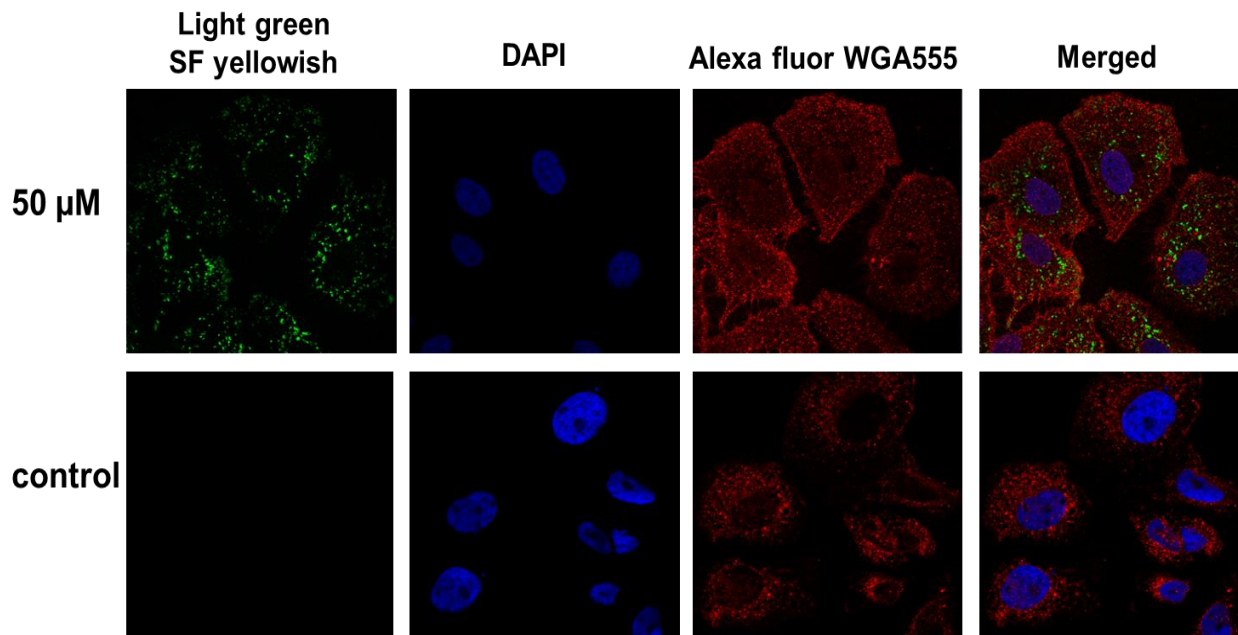


**Figure S5.** CLSM images of HeLa cells incubated in the presence of 50  $\mu\text{M}$  Light green SF yellowish for 24 hrs (upper row) compared to untreated cells incubated in the absence of compound (lower row). Alexa fluor WGA 555 was used to stain and indicate cell membranes, and DAPI was used to stain the nucleus. Bars represent 20  $\mu\text{m}$ .

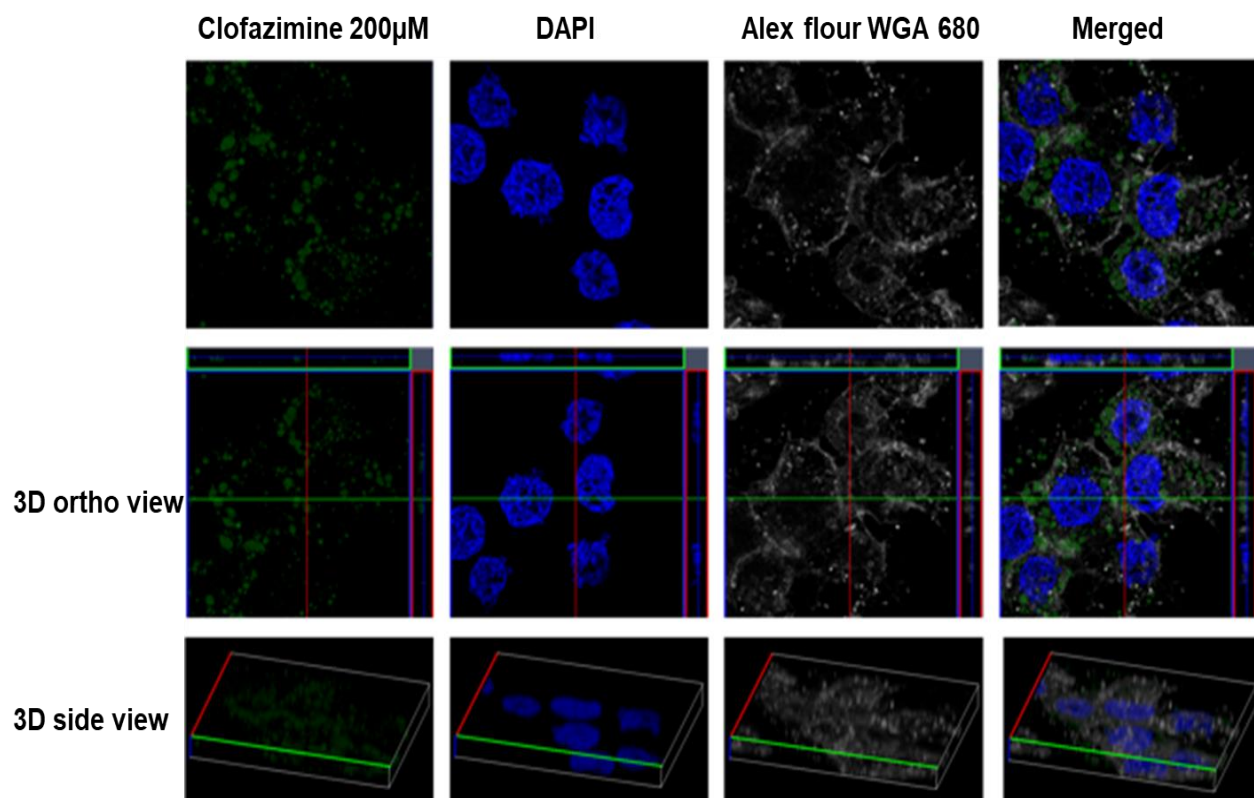
We observed that Light Green SF Yellowish is unstable after 24-48 hrs of incubation. Moreover, after the cell culture media was refreshed at the 24 hrs point, replaced with fresh-growth medium, (Figure S6) and then incubated for an additional 24 hrs, the compound aggregate nano-entities dissipated. CLSM analysis after 1, 3 and 5 hrs incubation did not reveal any visible aggregate formation. However, aggregates were readily visible after incubating the cells for 24 hrs in the presence of a 50  $\mu$ M drug compound. At the 24-hrs incubation point, visualization of the aggregate compound inside the cytoplasm demonstrated the stability of the compound in aggregate form. Alexa fluor WGA 555 and DAPI were used to stain the cells, as described previously.



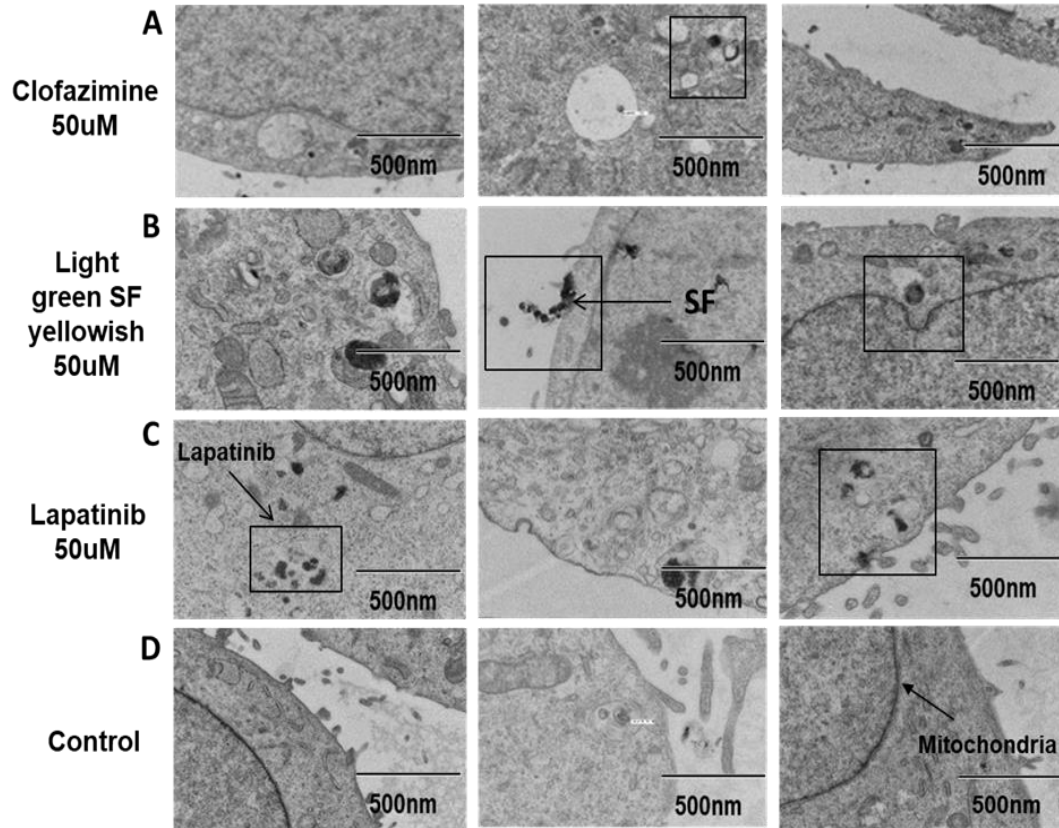
**Figure S6.** CLSM images of HeLa cells incubated in the presence of 50  $\mu$ M Light Green SF Yellowish for 24 hrs (top row) compared to untreated cells incubated in the absence of compound (middle row). The media were removed after 24 hrs, refreshed with new media, and then incubated for an additional 24 hrs (bottom row). Alexa fluor WGA 555 was used to stain and indicate cell membranes, and DAPI was used to stain the nucleus.



**Figure S7.** CLSM images of Huh-7 cells incubated in the presence of 50  $\mu$ M Light Green SF Yellowish for 24 hrs compared to untreated cells incubated in the absence of compound (bottom row). Alexa fluor WGA 555 was used to stain and indicate cell membranes, and DAPI was used to stain the nucleus.

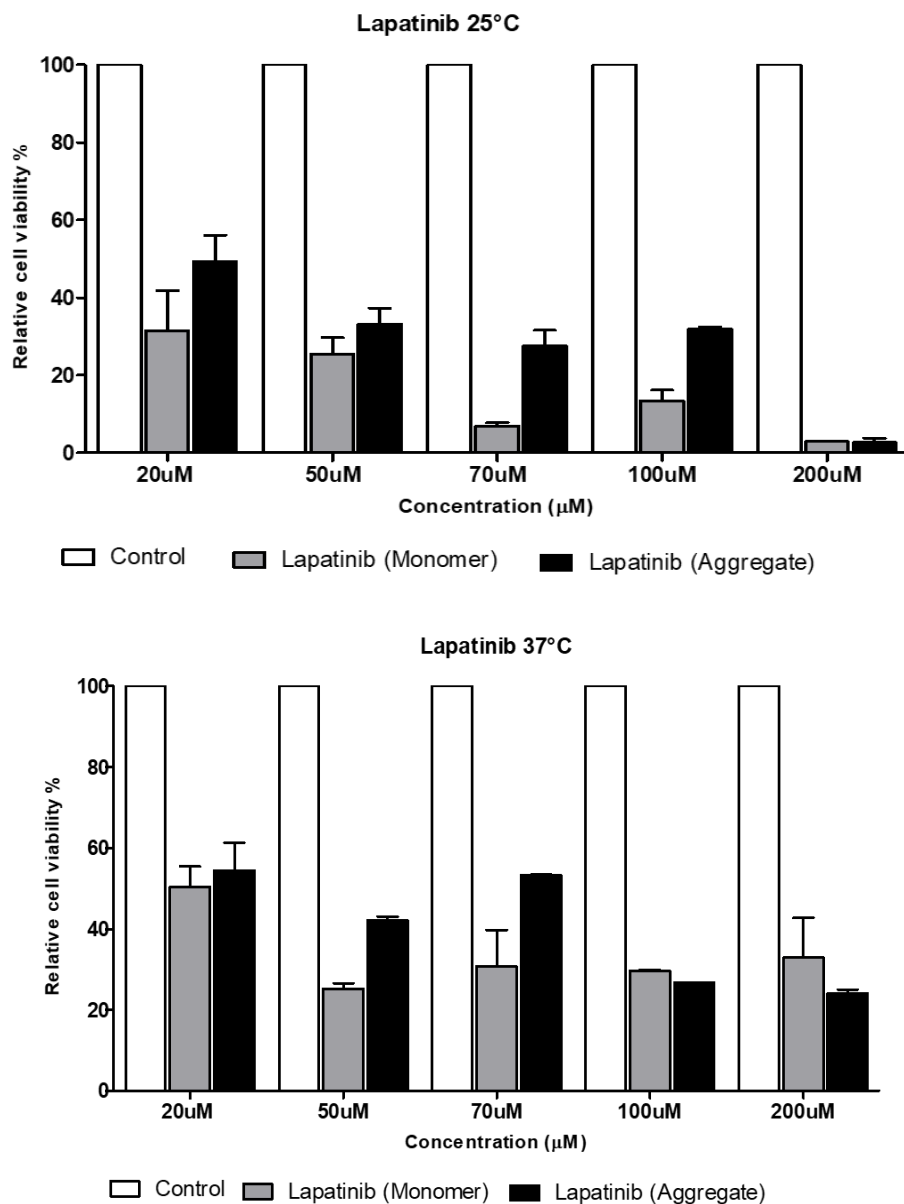


**Figure S8.** Confocal fluorescence microscopy of Huh-7 cells treated with Clofazimine at 200  $\mu$ M for 2 hrs (upper row), 3D ortho view (middle row), and 3D slide view (bottom row).



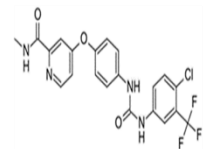
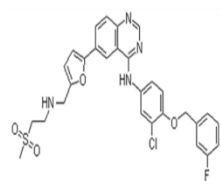
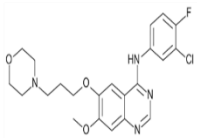
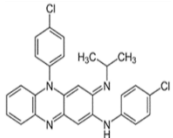
**Figure S9.** TEM images of cells incubated at 37 °C for 24 hrs and grown in the presence of (A) 50  $\mu$ M Clofazimine, (B) 50  $\mu$ M Light green SF yellowish, and (C) 50  $\mu$ M Lapatinib. (D) shows control cells grown in the absence of drugs. Bar represent 500 nm.

In the Figure below (MTT assay), cells were grown for 24 hours in the presence of 20, 50, 70, 100 and 200  $\mu\text{M}$  of Lapatinib in the presence and absence of 0.025% Tween 80. It was found that Lapatinib in the aggregate disassembled form (presence of 0.025% Tween 80) was much more potent as compared to the Lapatinib in its aggregate form (absence of 0.025% Tween 80). In our view, this simplistic test points to the idea that changing the aggregate attributes could alter properties and therefore more in-depth experiment are warranted.



**Figure S10.** Measurement of anti-proliferative activities of aggregate formation in contrast to the monomer form of Lapatinib at 25°C and 37° C, incubated in the presence and absence of 0.025% Tween 80. Two-way ANOVA ( $P < 0.05$ ).

**Table S1.** Evaluation of particle size and size distribution using dynamic light scattering (DLS). DLS was employed to evaluate particle size and distribution. The polydispersity index (PDI) is defined as a dimensionless measurement of the broadness of size distribution. The cumulant method for the analyzed DLS data was applied here. In the Zeta sizer software applications, the PDI usually has a specific range that varies from 0 to 1. Values greater than 1 indicate highly polydisperse distribution.

Drug Name	Structure	Size and Size Distribution Evaluation in Cell Culture Media			Size and Size Distribution Evaluation in Phosphate Buffer		PDI
		Aggregate Particle Size (d.nm)	Aggregate after Addition of Tween 80 (d.nm)	PDI	Aggregate Particle Size (d.nm)	Aggregate Size Following Addition of Tween 80 (d.nm)	
Sorafenib		164.2	13.54-15.69	0.457	220.2-255.0	8.721- 10.10	1.000
Lapatinib		255	10.10-11.70	0.158	164.2	255	0.172
Gefitinib		141.8-164.2	10.10	0.457	220-255.0	6.50-7.53	1.000
Clofazimine		295.3	164.2	0.457	220.2	21.4-24.36	1.000

**Table S2.** Small molecule compound aggregates shown in relation to aqueous conditions, particle size, shape, and molecular weight of drugs.

Compound (Indication) MW Structure	(g/mol)	Aqueous Conditions	Particle Size nm	Shape/Homogeneity
---------------------------------------	---------	--------------------	---------------------	-------------------

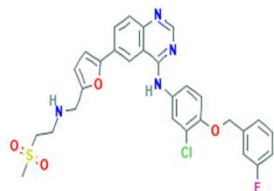
Lapatinib (anti-cancer)

581.06

50 mm phosphate buffer,  
Cell culture media

255

Spherical/  
homogeneous



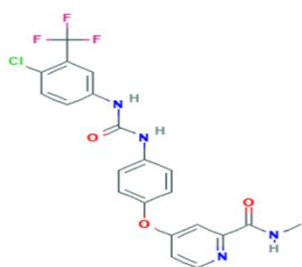
Sorafenib (anti-cancer)

637.0

50 mm phosphate buffer,  
Cell culture media

164.2

Spherical  
homogeneous

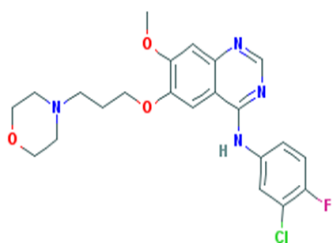


Gefitinib (anti-cancer)  
Crystal

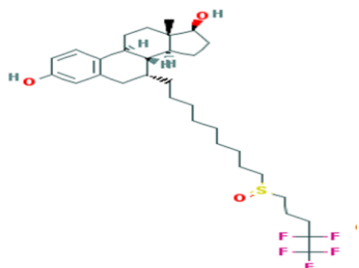
446.90

50 mm phosphate buffer,  
Cell culture media

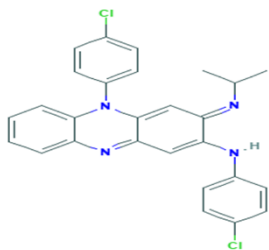
141.8-164.2



Fulvestrant (anti-cancer)      606.77      50 mm phosphate buffer,      —      Spherical/Crystal  
Cell culture media



Clofazimine  
(anti-leprosy)      473.40      50 mm phosphate buffer,      295.3      Spherical  
Cell culture media      homogeneous



## **CHAPTER 4: RÉSUMÉ EN FRANÇAIS**

## 4.1 Introduction

Lorsque des composés sont placés en milieu aqueux, il est communément admis qu'ils peuvent se solubiliser et se disperser dans une solution et /ou se précipiter. Toutefois, cet état biphasique n'est plus valide. Il existerait plutôt un modèle triphasique qui décrit mieux le comportement de composés en solution. Selon un tel modèle, des composés peuvent également adopter une phase intermédiaire où ceux-ci s'auto-associent en structure pouvant ressembler à des grappes, des fibres, des micelles et de nombreuses autres formes. Bien que les paramètres physicochimiques qui dictent les caractéristiques de ces assemblages ne soient pas encore compris, il est clair que la nature triphasique des composés affecte profondément ses propriétés, en particulier du point de vue pharmaceutique. Nous appelons ces assemblages des «nano-entités» et qui seront discutés dans l'introduction (Chapitre 1).

Cette thèse vise à attirer l'attention sur ces nano-entités qui, pour la plupart, sont difficilement détectables parce qu'elles sont invisibles à l'œil nu et que les stratégies de détection sont sous-développées. Nous avons utilisé la résonance magnétique nucléaire (RMN) pour détecter les agrégats, qui consiste à surveiller le comportement en solution d'une série des petits colorants à différentes concentrations (voir le chapitre 2). Cet essai démontre que certains colorants peuvent exister sous forme soluble, tandis que d'autres peuvent adopter des agrégats de différentes tailles. Il est intéressant de noter que les colorants ayant des structures chimiques très similaires peuvent adopter des agrégats de tailles très différentes - démontrant l'existence de relations structure-nano-entité - suggérant qu'ils peuvent être conçus pour avoir des propriétés distinctes. Une propriété a été évaluée où le médicament, la quétiapine (Seroquel), a été ajouté au colorant rouge Congo, ce qui a entraîné l'absorption du médicament dans la nano-entité du colorant. Cela montrait une interaction directe médicament-colorant et démontrait que les agrégats de colorant pouvaient avoir une influence sur le comportement de médicament dans la solution. En résumé, nos études démontrent que le test d'agrégation par RMN peut constituer un outil pratique et précieux pour évaluer les nano-entités et mieux comprendre leurs propriétés (par exemple, la toxicité, l'activité non ciblée) et leur utilité potentielle comme l'encapsulation et l'administration de médicaments systémiques.

Le chapitre 3 explore plus en détail les stratégies complémentaires de détection des nano-entités. L'objectif était de développer, autant que possible, une combinaison de méthodes pouvant ensuite être utilisées pour corréler les propriétés d'un composé à son comportement physicochimique et à celui d'une nano-entité en solution. Nous utilisons plusieurs médicaments anticancéreux (Sorafenib, Lapatinib, Gefitinib et Fulvestrant) et un médicament neuroactif, la Clofazimine comme modèles afin de mieux comprendre leur comportement physico-chimique et leurs propriétés d'auto-association, ainsi que d'explorer diverses techniques pour explorer leur équilibre au sein du modèle en trois états. Leurs comportements dans les tampons, les milieux et les cellules ont été évalués par une combinaison de RMN, de diffusion dynamique de la lumière (DLS), de microscopie électronique à transmission (TEM) et de microscopie confocale. On a découvert que ces médicaments s'associaient eux-mêmes à des nano-entités relativement grandes de types et des tailles distincts qui dépendaient du milieu où ils se trouvent. De plus, ces composés étaient capables de pénétrer à l'intérieur de cellules. Des avantages remarquables et des désavantages ont été observés pour les différentes techniques de détection utilisées. Il a été conclu qu'une combinaison de méthodes était nécessaire pour exposer l'équilibre de ces médicaments en solution.

Enfin et à partir des travaux ci-dessus, nous pensons que ces petites molécules peuvent former de nombreux types de nano-entités qui dépendent des milieux et des conditions. Ces entités ont des propriétés - certaines indésirables et d'autres favorables. Nos stratégies peuvent aider à la détection de ces entités. Ces derniers pourraient donc être utilisés comme systèmes d'encapsulation et d'administration de médicaments.

Cette thèse vise à modifier la vision biphasique commune des molécules/composés en solution en une vision plus triphasique incluant une phase d'agrégat intermédiaire. Les agrégats peuvent se former spontanément et de manière réversible dans un tampon aqueux, ce qui réfère à une concentration critique d'agrégation (CAC) (Duan et al., 2015; Irwin et al., 2015). Chaque composé possède sa propre empreinte dans ce modèle triphasique, qui dépend du solvant, du milieu, de la concentration, de la température, du pH et de nombreux autres facteurs. L'existence d'agrégats solubles, leurs variations de tailles et de types et leurs propriétés ont longtemps échappé à la détection et à l'attention des chercheurs. L'agrégation de petites molécules peut se former dans des milieux aqueux à des concentrations d'ordre micromolaires et même sous-micromolaires allant de 50 à plus de 800 nm (Owen et al., 2012). De plus, l'agrégation est stable dans les milieux du système biologique tels que le tractus gastro-intestinal et l'intestin, ainsi que dans le milieu riche en albumine (Tóth et al., 2017) (Lu et al., 2011). Les travaux précédents ont souvent été rationalisés sur la base des observations selon lesquelles des composés médicamenteux typiques sont fortement liés au sérum *in vivo* (Lu et al., 2011). Pour cette raison, on s'attendrait à ce que la majorité des composés soient liés aux protéines sériques telles que l'albumine, ce qui ne permet pas aux composés de s'auto-associer. Cette hypothèse s'avère toutefois non-fondée puisque dans une étude précédente impliquant un test d'agrégation par RMN, il a été clairement démontré que les composés agrégateurs restaient auto-associés dans une gamme de tampons pharmacologiques, plasmatiques et sanguins. Cela suggère qu'il existe une propension significative pour l'auto-association de certains composés (LaPlante et al., 2013).

Les agrégats peuvent avoir des propriétés particulières qui peuvent changer leur cible et ainsi biaiser les résultats. Celles-ci peuvent engendrer des faux-positifs qui pourrait être liés à la réactivité chimique, à la flexibilité moléculaire élevée et à l'hydrophobicité du composé (Feng et al., 2005). En outre, la relation structure-activité (SAR) pourrait également contribuer à ce phénomène. Par exemple, certains colorants ayant des structures très similaires peuvent générer des agrégats de taille très différentes (Murugesan et al., 2018). Des études précédentes ont également signalé que l'agrégation peut entraîner des résultats biaisés grâce à une inhibition non-spécifique (Irwin et al., 2015). D'autres études suggèrent aussi que les agrégats ont des propriétés qui y sont associées et qui pourraient avoir des impacts sur le processus de développement des

médicaments. Par exemple, une étude systématique a montré que 95% des résultats d'un criblage à haut débit étaient éliminés en tant que faux positifs en raison de la formation des agrégats (Feng et al., 2007). Cependant, les études à ce jour viennent tout juste de commencer à corrélérer l'existence de nano-entités avec la toxicité des médicaments et l'hyper-biodisponibilité. Ils peuvent également entraîner des interactions non spécifiques avec diverses protéines, ce qui conduit à des tests de criblage non fiables. En fait, certaines molécules (médicaments) inhibent de nombreuses enzymes. Malgré les études menées sur ces mécanismes, il existe encore une population d'inhibiteurs d'enzymes non spécifiques mal compris. Il a été découvert précédemment que des molécules non apparentées partageaient plusieurs propriétés inhabituelles, telles qu'un comportement dépendant du temps, des courbes d'inhibition prononcées, une sensibilité à la concentration en enzyme et à la force ionique. Pour expliquer ce comportement, il a été suggéré que ces composés partagent la capacité de former des agrégats à des concentrations de l'ordre du micromolaire en solution aqueuse et que l'inhibition de diverses enzymes est provoquée par ces espèces d'agrégats (Seidler et al., 2003), ce qui pourrait biaiser les résultats dans les essais biochimiques. Néanmoins, la manière dont les agrégats provoquent une inhibition non spécifique reste mal comprise.

#### **4.2 Méthodes de détection de l'agrégation de composés**

Plusieurs méthodes informatiques et tests biophysiques sont actuellement utilisés pour détecter des agrégats de petites molécules en solution aqueuse. L'une des méthodes les plus courantes consiste en des tests d'inhibition enzymatiques, tels que la lactate déshydrogénase, la  $\beta$ -lactamase et la chymotrypsine, largement utilisés pour identifier l'agrégation en mesurant l'absorbance des modifications colorimétriques des produits de réaction enzymatiques. Avec la présence d'une agrégation et d'une inhibition non spécifique des protéines, le rapport de réaction enzymatique et la cinétique de la réaction pourraient être altérés. De plus, les changements colorimétriques permettent l'observation directe et la lecture de l'activité enzymatique. Cependant, l'absorbance de petites molécules pourrait influencer le signal final d'absorbance sans tenir compte de la possibilité de former des agrégats potentiels. D'autres méthodes courantes incluent la diffusion dynamique de la lumière (DLS) qui est une méthode de détection relativement simple. Elle est utilisée pour évaluer la taille des agrégats en suspension dans une solution en déterminant les fluctuations temporelles déterminées par l'intensité de la diffusion. Cependant, la caractérisation de l'agrégation

de médicament par ces méthodes a été limitée en raison de l'absence de simplicité et de fiabilité. De plus, le DLS pourrait être sensible aux gros agrégats mais est moins idéal pour caractériser des petites entités, et certains pensent qu'il est vraiment difficile de différencier les agrégats des précipités à l'aide de ce test. La résonance plasmonique de surface (SPR) est une autre méthode de détection d'agrégats récemment utilisée sur une surface de biocapteur optique. Dans cet essai, la simplicité apparaît dans la différenciation entre l'affinité de liaison et l'agrégation du composé. Le SPR est donc considéré comme plus fiable par rapport aux méthodes d'inhibition enzymatique ou DLS en raison de sa mesure directe de l'affinité des molécules observées.

Très récemment, des agrégats des composés dans des milieux aqueux ont été détectés en effectuant un essai de  $^1\text{H}$ -RMN au moyen de diverses expériences de dilution. En utilisant ce test, l'élimination des molécules agrégées des bibliothèques de criblage de fragments serait plus simple. Un grand nombre de petites molécules sont affectées par une agrégation qui existe plus probablement à des concentrations élevées. Tel que décrit précédemment, lorsqu'un composé est placé dans un milieu aqueux, il est supposé adopter un équilibre entre trois phases différentes, notamment les formes solides, solubles et les d'agrégats solubles. Chaque phase individuelle de ces trois états peut être identifiée de manière significative par  $^1\text{H}$ -RMN. Il est à noter que plusieurs composés présentent des spectres de  $^1\text{H}$ -RMN normaux, alors que d'autres présentent des spectres inhabituels. De plus, les résonances de RMN pourraient être aiguës ou larges en fonction des comportements globaux de culbutage de chaque état. Une résonance RMN nette devrait être observée pour les molécules simples solubles en raison de leurs culbutage rapide (*fast-tumbling behaviors*). Par contre, les formes solides ne seront probablement pas observées par RMN en raison de leurs culbutage lent (*slow-tumbling behaviors*). Cependant, les gros agrégats peuvent également être détectés à l'aide du spectre de RMN, mais nécessitent la décomposition des agrégats en entités plus petites en utilisant des détergents à des fins de détection.

### **4.3 Hypothèse**

Notre hypothèse est que de nombreux types de nano-entités médicamenteuses existent et sont détectables. En outre, plusieurs types de molécules médicamenteuses et de colorants manifestent des processus d'agrégation et ont la capacité de pénétrer membranes cellulaires.

### **4.4 Objectifs**

#### **4.4.1 Développer des techniques efficaces pour détecter l'ensemble des nano-entités**

Nous développons d'abord une série d'essais et de stratégies d'agrégation accessibles et complémentaires. Pour ce faire, les outils scientifiques doivent être systématiquement évalués, dans le but de permettre la détection de l'ensemble des types et tailles de nano-entités. Chaque technique ayant ses points forts et ses points faibles. Nous avons l'intention d'acquérir des données sur un ensemble de produits connus pour être des agrégateurs ou des non-agrégateurs. En outre, afin de bien observer et caractériser les agrégats de petite et moyenne taille, divers outils ont été explorés (tests d'agrégation de  $^1\text{H}$ -RMN) susceptibles d'être soumis à un criblage à haut débit. Bien que cela ne soit pas idéal, de très grands agrégats invisibles à la RMN peuvent être exposés et observés par  $^1\text{H}$ -RMN suite à un ajout de détergents. Parmi les autres solutions permettant d'observer directement de gros agrégats, citons les techniques de diffusion dynamique de la lumière (DLS), qui peuvent indiquer la taille des gros agrégats, mais sont peu pratiques pour les mélanges d'agrégats et surtout les petits agrégats. Ainsi, comme la microscopie électronique peut fournir des informations visuelles détaillées sur les grands agrégats (tailles et types), cette approche a été utilisée pour des composés sélectionnés.

#### **4.4.2 Démontrer la capacité de l'agrégation de petites molécules à pénétrer dans la membrane cellulaire et étudier leur effet sur la prolifération cellulaire.**

Les composés agrégateurs sont réputés pour leur présence dans les cellules et les noyaux, ce qui pourrait entraîner des faux-positifs lors de criblage des composés à l'aide de tests biochimiques. Cependant, on connaît très peu de choses sur la manière dont les agrégats entrent dans la cellule, bien que certaines hypothèses aient été proposées. Nous menons des expériences pour mieux comprendre l'existence d'agrégats à l'intérieur des cellules, dont les résultats devraient ensuite

éclairer leur mécanisme d'action. Des études antérieures sur les effets toxiques dans les cellules indiquent que les composés en agrégation ont tendance à provoquer des effets indésirables tels que des éruptions cutanées graves chez les modèles animaux. Cet objectif a évalué l'impact des agrégats pénétrant dans les cellules et les noyaux et affectant les organites. Les propriétés de réponse à la toxicité ont également été évaluées. La microscopie confocale a été utilisée pour détecter les agrégats de composés fluorescents. En appliquant cette approche, nous pourrions voir l'agrégation à l'intérieur des cellules, des noyaux et du cytoplasme.

## REFERENCES

1. Chan LL, Lidstone EA, Finch KE, Heeres JT, Hergenrother PJ & Cunningham BT (2009) A method for identifying small-molecule aggregators using photonic crystal biosensor microplates. *JALA: Journal of the Association for Laboratory Automation* 14(6):348-359.
2. Coan KE, Maltby DA, Burlingame AL & Shoichet BK (2009) Promiscuous aggregate-based inhibitors promote enzyme unfolding. *J. Med. Chem.* 52(7):2067-2075.
3. Duan D, Doak AK, Nedyalkova L & Shoichet BK (2015) Colloidal aggregation and the in vitro activity of traditional Chinese medicines. *ACS Chem. Biol.* 10(4):978-988.
4. Feng BY, Shelat A, Doman TN, Guy RK & Shoichet BK (2005) High-throughput assays for promiscuous inhibitors. *Nat. Chem. Biol.* 1(3):146.
5. Feng BY, Simeonov A, Jadhav A, Babaoglu K, Inglese J, Shoichet BK & Austin CP (2007) A high-throughput screen for aggregation-based inhibition in a large compound library. *J. Med. Chem.* 50(10):2385-2390.
6. Irwin JJ, Duan D, Torosyan H, Doak AK, Ziebart KT, Sterling T, Tumanian G & Shoichet BK (2015) An aggregation advisor for ligand discovery. *J. Med. Chem.* 58(17):7076-7087.
7. LaPlante SR, Aubry N, Bolger G, Bonneau P, Carson R, Coulombe R, Sturino C & Beaulieu PL (2013a) Monitoring drug self-aggregation and potential for promiscuity in off-target in vitro pharmacology screens by a practical NMR strategy. *J. Med. Chem.* 56(17):7073-7083.
8. LaPlante SR, Carson R, Gillard J, Aubry N, Coulombe R, Bordeleau S, Bonneau P, Little M, O'Meara J & Beaulieu PL (2013b) Compound aggregation in drug discovery: implementing a practical NMR assay for medicinal chemists. *J. Med. Chem.* 56(12):5142-5150.
9. Lu J, Owen SC & Shoichet MS (2011) Stability of self-assembled polymeric micelles in serum. *Macromolecules* 44(15):6002-6008.
10. Murugesan JR, Shahout F, Dlim M, Langella MM, Cuadra-Foy E, Forgione P & LaPlante SR (2018) Revealing dye and dye-drug aggregation into nano-entities using NMR. *Dyes and Pigments* 153:300-306.
11. Owen SC, Doak AK, Wassam P, Shoichet MS & Shoichet BK (2012) Colloidal aggregation affects the efficacy of anticancer drugs in cell culture. *ACS Chem. Biol.* 7(8):1429-1435.

12. Seidler J, McGovern SL, Doman TN & Shoichet BK (2003) Identification and prediction of promiscuous aggregating inhibitors among known drugs. *J. Med. Chem.* 46(21):4477-4486.
13. Tóth G, Jánoska Á, Völgyi G, Szabó Z-I, Orgován G, Mirzahosseini A & Noszál B (2017) Physicochemical characterization and cyclodextrin complexation of the anticancer drug lapatinib. *Journal of Chemistry* 2017, 4537632.